

In Search of Adam’s Secret Sauce

Antonio Orvieto *

ELLIS Institute Tübingen, MPI-IS
Tübingen AI Center, Germany

Robert Gower

Flatiron Institute
New York, US

Abstract

Understanding the remarkable efficacy of Adam when training transformer-based language models has become a central research topic within the optimization community. To gain deeper insights, several simplifications of Adam have been proposed, such as the signed gradient and signed momentum methods. In this work, we conduct an extensive empirical study — training over 1,300 language models across different data configurations and scales — comparing Adam to several known simplified variants. We find that signed momentum methods are faster than SGD, but consistently underperform relative to Adam, even after careful tuning of momentum, clipping setting and learning rates. However, our analysis reveals a compelling option that preserves near-optimal performance while allowing for new insightful reformulations: constraining the Adam momentum parameters to be equal, $\beta_1 = \beta_2$. Beyond robust performance, this choice affords new theoretical insights, highlights the “secret sauce” on top of signed momentum, and grants a precise statistical interpretation: we show that Adam in this setting implements a natural online algorithm for estimating the mean and variance of gradients—one that arises from a mean-field Gaussian variational inference perspective.

1 Introduction

Despite a decade of research into efficient and performant adaptive optimizers for deep learning, the *de facto* choice for large-scale training today remains Adam [Kingma and Ba, 2014], especially for training language models (LMs) [Grattafiori et al., 2024, Liu et al., 2024]. At the root of this choice is the peculiar geometry of optimization landscapes induced by the transformer architecture [Noci et al., 2022, Zhang et al., 2024a], as well as the noisy/unbalanced nature of tokenized text data [Zhang et al., 2020a, Kunstner et al., 2024].

In recent years, the surge of extremely large-scale and expensive-to-pretrain language models has further pushed the community to better understand Adam’s performance and to propose faster, efficient, and robust alternatives. Towards achieving this goal, contemporary studies [Kunstner et al., 2023, Bernstein and Newhouse, 2024] have brought up a close similarity between the performance of Adam and SignSGD [Bernstein et al., 2018] with momentum. While such results are extremely valuable to forward our understanding, they are not precise enough: already at a scale of 160M parameters we found that extensive tuning of Signum (SignSGD with momentum), while closing 96% of the perplexity gap between SGD and Adam, results in a 25% effective slowdown (Figure 1).

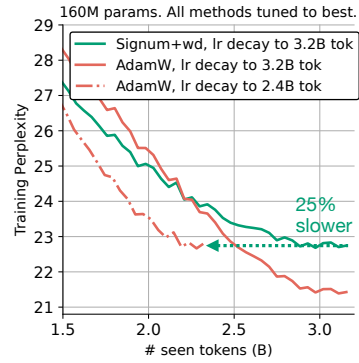


Figure 1: *Pretraining on SlimPajama with Chinchilla-optimal [Hoffmann et al., 2022] scaling.* Both momentum and learning rates for *Signum* are extensively tuned (§3). While *Signum* closes 96% of the perplexity gap between Adam and SGD with momentum (Table 1), still results in a 25% slowdown: Adam achieves the same performance with 3/4 of the budget.

* antonio@tue.ellis.eu.

Table 1: (**Signum closes 96% of the perplexity gap between Adam and SGD**) Validation perplexity comparison of widely used optimizers that interpolate between SGD and Adam, evaluated on a language modeling task (160M parameters, 3.2B SlimPajama tokens, sequence length 2048, batch size 256 – Chinchilla optimal). We report the mean and 2-sigma interval of validation perplexity (on 100M held-out tokens) across 3 initialization seeds. Weight decay is always decoupled [Loshchilov and Hutter, 2019] and set to 0.1 [Biderman et al., 2023, Liu et al., 2024] except for SGD where we further tune (SB). RMSprop does not use momentum, and Gclip is global norm clipping to 1 (before applying momentum), Cclip is coordinate-wise clipping (after applying momentum). Other hyperparameters, for all other methods, are carefully tuned, see e.g. Figure 2 and §3.

To optimally tune hyperparameters (e.g. Figure 2), we performed a total of 582 full training runs.

	Adam	Signum	RMSprop	SGD+Cclip	SignSGD	SGD+Gclip	SGD
Val ppl.	21.86 ± 0.21	23.23 ± 0.16	27.04 ± 0.34	33.40 ± 0.39	36.78 ± 0.57	37.76 ± 0.61	53.62 ± 5.14

While for large-scale training, the slowdown in Figure 1 is not acceptable, it may seem unnecessary or anachronistic to further explain it, in light of recent algorithms claiming to have further improved the performance of Adam, e.g. Muon [Jordan et al., 2024, Liu et al., 2025, Shah et al., 2025], Scion [Pethick et al., 2025], and Shampoo-based [Gupta et al., 2018] methods such as SOAP [Vyas et al., 2025]. However, a close inspection of such optimizers reveals that, while gains over vanilla Adam are solid, *those are contingent on the use/adaptation of Adam on a specific subset of parameters*: For instance, in recent scaled-up versions of Muon [Liu et al., 2025, Shah et al., 2025], Adam is used to update embedding, LM heads and normalization parameters², and on the other parameters the Muon update is normalized to have a similar RMS value similar to the Adam update. Further, SOAP’s improvements stem from the application of Adam in the preconditioner’s eigenbasis.

The discussion above and the results in Figure 1 inspires us to further dissect – once again [Balles and Hennig, 2018] – the mechanisms of Adam compared to those of simpler methods in language modeling with transformers.

Towards improving our understanding of Adam, we make the following contributions:

- We perform a large-scale evaluation (~ 10 thousand NVIDIA A100-SXM4-80GB GPU hours) of the performance of established algorithms which claim a theoretical or empirical similarity/dissimilarity with Adam on 160M parameters LMs with usual configurations [Biderman et al., 2023, Black et al., 2022], at a compute-optimal budget on different datasets, at different batch-sizes and sequence lengths (up to 2048 tokens). Crucially, we sweep over all momentum parameters for each method, for each learning rate in our grid – for each of our settings. We find that, while clipping and sign descent methods can close most of the gap with SGD, their performance is not satisfactory in comparison to Adam (Figure 2). We make all of our data, e.g. loss dynamics for all our settings, publicly available at <https://github.com/aorvieto/SecretSauce>.
- Through our extensive tuning of Adam (e.g., Figure 2, comprising 200 distinct hyperparameter settings), we identify one simplification that does perform well: that of setting $\beta_1 = \beta_2$ (emerging practical choice in contemporary literature [Zhao et al., 2025, Shah et al., 2025, Cattaneo and Shigida, 2025, Zhang et al., 2025]). We validate this finding (§3.2) at different batchsizes, data source, token budget, sequence length and larger scale (410M): $\beta_1 = \beta_2$ performs at near-optimality across the majority of our experiments, see Figure 3. Given the breadth of our evaluation and the robustness of this finding, we recommend adopting $\beta_1 = \beta_2$ as the default setting for Adam for training language models at similar data and parameter scales. More broadly, this perspective suggests that Adam can be effectively treated as a one-parameter optimizer (as Signum).
- We show in §4, that reducing $\beta_1 = \beta_2 = \beta$ to a single parameter, leads to a surprising new interpretation of Adam: it is built on top of a nontrivial yet principled online method for estimating mean and variance of the gradients. Indeed, we can view the two momentum buffers as the result of an online Gaussian Variational inference method for tracking the mean and variance of the gradients as they change across iterations. This viewpoint directly adds to the discussion by Balles and Hennig [2018], yet affords more precision induced by our empirically-informed simplification.
- We offer a toy quadratic example illustrative of our findings, building on top of recent works on the peculiar landscape of transformer-based language modeling problems [Noci et al., 2022, Zhang et al., 2024a]. This example replicates the gaps between tuned SGD, Signum, and Adam with equal betas in a 9-dimensional setting, helpful for future research and to gain intuition.

²Coincidentally, the ones that were shown to be most sensitive during training [Zhao et al., 2025, Kunstner et al., 2024]. Scion, claiming a greater independence from Adam, adopts an architecture where normalization layers have no gain parameters.

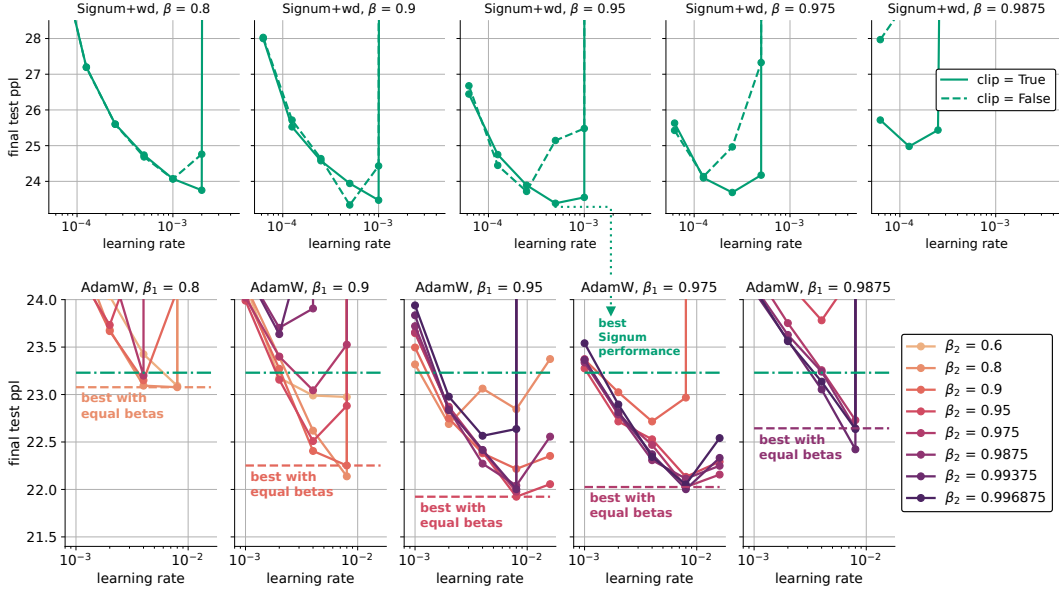


Figure 2: Training a total of 265 language models with 160M parameters with 3.2B SlimPajama-627B tokens, sequence length of 2048, batch size of 256. Shown is the final test perplexity on 100M held-out tokens. Some underperforming runs are not shown to keep focus on the most interesting range. For a careful description of our tuning grid, see §A. **Takeaway 1:** Validation perplexity of highly tuned (65 hyperparameter configurations) *Signum* with weight decay 0.1 – top row – is around 23.23 (see Table 1 for multiple seeds at optimal tuning). We ablate on the momentum parameter, learning rate, and presence of global clipping before averaging. The best performance of *Signum* is reported as a green horizontal line on the second row (200 Adam runs, with weight decay of 0.1). Most Adam runs perform better than optimally tuned *Signum*. **Takeaway 2:** For each β_1 , the optimal corresponding β_2 (after learning rate tuning) is similar. The higher β_1 , the higher β_2 for optimal performance (optimal β s are correlated).

2 Preliminaries and Related Works

For a signal $(s_k)_{k \in \mathbb{N}}$ and $\beta \in [0, 1]$, we define the β -normalized exponential moving average:

$$\text{EMA}_\beta[s_k] = \beta \text{EMA}_\beta[s_{k-1}] + (1 - \beta)s_k, \quad \text{EMA}_\beta[s_0] := s_0 \text{ (or zero).} \quad (1)$$

The Adam optimizer [Kingma and Ba, 2014] without bias correction³ takes the following form:

$$w_{k+1} = w_k - \eta_k \left(\sqrt{\text{EMA}_{\beta_2}[g_k^2]} + \epsilon \right)^{-1} \text{EMA}_{\beta_1}[g_k] \quad (\text{Adam})$$

where all division and multiplications are element-wise, $w_k, g_k \in \mathbb{R}^d$ are model parameters and gradients at iteration k , η_k is the scheduled learning rate, and $\epsilon > 0$ is a small constant. RMSprop [Tieleman and Hinton, 2012] is an earlier method that sets $\beta_1 = 0$.

One special case, and simplification, of Adam is to consider $\beta_1 = \beta_2 = \epsilon = 0$ which gives SignSGD:

$$w_{k+1} = w_k - \eta_k \text{sign}[g_k]. \quad (\text{SignSGD})$$

A practical variant of SignSGD, which has shown strong performance in language modeling [Kunstner et al., 2023], first computes an exponential moving average (EMA) – or momentum – of the gradients before applying the sign operator [Bernstein et al., 2018]:

$$w_{k+1} = w_k - \eta_k \text{sign}[\text{EMA}_\beta[g_k]]. \quad (\text{Signum})$$

In practice, every language modeling pipeline (see e.g. [Karpfathy, 2022]) incorporates some gradient clipping strategy [Pascanu et al., 2013], a component known to stabilize training in the autoregressive

³We show in Table 3 that the presence of bias correction does not affect our results at the best hyperparameter configuration. However, for all our runs, we use the Pytorch implementation including this factor, for simplicity.

setting and to make gradients more robust to the stochasticity of language [Zhang et al., 2020b]. Global norm clipping (that we abbreviate Gclip), processes gradients fresh out of the backward pass:

$$\text{clip}[g_k] = \min \left\{ 1, \frac{1}{\|g_k\|_2} \right\} g_k.$$

In our experiments, we start from vanilla SGD with momentum: $w_{k+1} = w_k - \eta_k \text{EMA}_\beta[g_k]$ and ablate on the positive effect of Gclip before applying momentum. Regarding coordinate clipping (Cclip), a softer version of sign, we consider applying it to $\text{EMA}_\beta[g_k]$ – in connection with Signum.

Research on Adam, a short summary. Despite initial concerns on generalization [Wilson et al., 2017] and convergence [Reddi et al., 2018], after the introduction of decoupled weight decay (i.e., AdamW [Loshchilov and Hutter, 2019]) Adam rapidly became the de-facto standard optimizer in deep learning, with works highlighting its landscape adaptation properties [Orvieto et al., 2022] and its debated connections to empirical Fisher preconditioning [Kunstner et al., 2019].

With the advent of Transformers [Vaswani et al., 2017], early works noticed an intriguing gap with SGD performance in language modeling [Xiong et al., 2020] (much larger than what can be observed, e.g., in CNNs on image data), that was initially attributed to heavy-tail noise in text data [Simsekli et al., 2019, Zhang et al., 2020a] – suggesting Adam performance to be correlated with its adaptive coordinate clipping mechanism [Zhang et al., 2020a].

As models became larger and more hardware-demanding, interest spiked in the community to reduce the memory footprint of Adam [Li et al., 2023, Zhang et al., 2024b] and to search for more efficient options [Chen et al., 2023, Liu et al., 2023]. Current trends, draw an intriguing connection between Adam and SignSGD [Bernstein and Newhouse, 2024], and in particular with its momentum variant: Signum [Bernstein et al., 2018]. This connection was first suggested in early attempts to understand Adam’s empirical performance [Balles and Hennig, 2018], and has recently gained renewed attention in light of transformer architectures and their heterogeneous optimization landscapes [Noci et al., 2022, Zhang et al., 2024a, Tomihari and Sato, 2025, Kunstner et al., 2024, Zhao et al., 2025]. These landscape-based arguments are now more compelling, as recent evidence shows that Adam and signed momentum methods outperform SGD even in deterministic settings [Kunstner et al., 2023].

Our approach. Although recent literature highlights many connections between Adam and simpler methods such as Signum—which involve fewer hyperparameters, the computational demands of thoroughly studying Adam on small- to medium-scale language models remain prohibitive for most academic optimization researchers. This challenge is amplified by the combinatorial explosion of hyperparameter configurations required for rigorous comparisons. In §3, we aim to provide a comprehensive empirical reference for optimizer performance across a range of language modeling settings. Our key findings are distilled into two main takeaways (Figure 2), which are further supported by theoretical insights in §4.

3 Experiments

In our experiments, we systematically explore Transformer-based language models using a nanoGPT [Karpathy, 2022] implementation⁴ enhanced by recent advancements such as Rotational Positional Embeddings [Su et al., 2024], RMSNorm normalization [Zhang and Sennrich, 2019], and SwiGLU activation functions [Shazeer, 2020]. We adopt a robust training protocol inspired by successful practices established in large language models like LLaMa [Touvron et al., 2023], GPT-neox [Black et al., 2022], GPT-J [Wang and Komatsuzaki, 2022] and Pythia [Biderman et al., 2023], leveraging techniques including bfloat16 precision, linear warm-up followed by a cosine annealing schedule [Loshchilov and Hutter, 2016], and global gradient norm clipping (unless specified). Our model configurations follow [Biderman et al., 2023] and are presented, alongside a detailed description of all tuning settings and resources, in §A.

3.1 Extensive benchmarking at 160M parameters

We conduct 475 compute-optimal pretraining runs on the SlimPajama-627B dataset [Soboleva et al., 2023], using a sequence length of 2048, a batch size of 256, and a decoupled weight decay of 0.1 [Loshchilov and Hutter, 2019] (except for SGD). We always report validation perplexity on a

⁴<https://github.com/Niccolò-Ajroldi/plainLM/tree/main>

held-out subset of 100M tokens. Results from these tuning sweeps are summarized in Table 1, Figure 2, and Appendix B.1. The runs span the following configurations:

- SGD (131 runs): Tuned parameters include weight decay (too large causes instability), global norm clipping (Gclip). We also consider clipping coordinates after applying momentum (Cclip). For all these options, momentum and learning rates are independently tuned.
- RMSprop (48 runs): Tuned parameters include momentum on the preconditioner and learning rate.
- Signum (70 runs): Tuned parameters include global norm clipping, momentum, and learning rate.
- Momentum on SignSGD (35 runs): This variant inverts the order of the sign and EMA operations (and performs worse than Signum). Clipping has no effect here due to the sign operation.
- AdamW (200 runs): Tuned parameters include both momentum terms and the learning rate.

Two additional seeds are provided for the best performing hyperparameter settings, see Table 1.

Choice for betas grid. While we vary the learning rate by powers of two, our choice of moving average parameters is guided by recent insights into Adam scaling behavior [Malladi et al., 2022, Compagnoni et al., 2025]: we choose $\beta = 1 - \kappa(1 - \beta_{\text{base}})$ where $\beta_{\text{base}} = 0.9$ and $\kappa \in \{2^{-5}, 2^{-4}, \dots, 2^2\}$. This makes it such that the accumulation factor $1/(1 - \beta) = 1/(\kappa(1 - \beta_{\text{base}}))$.

Takeaway 1. As shown in Figure 2 and Table 1, optimally tuning Signum with weight decay leads to significant improvements over standard SGD, in line with recent findings [Kunstner et al., 2023, Zhao et al., 2025]. Nonetheless, Adam consistently outperforms the alternatives across most settings, suggesting that it retains a key advantage—a "secret sauce"—that continues to set it apart from better-understood methods in large-scale optimization tasks.

This gap is not limited to this specific setup. In §3.2 we discuss results on another dataset (Fineweb), with disabled weight decay, and shorter sequence lengths. Further, we ablate on other potential confounders (initialization of moving averages, bias corrections, Adam ϵ value) in §3.3.

Takeaway 2 (a). In Figure 2, we clearly see that $\beta_1 = \beta_2$ yields near-optimal performance in Adam, for the five β_1 values we considered. In § 3.2 we show similar results at different batch sizes, different sequence lengths, and with disabled weight decay on a different dataset. We also extend this observation to 410M parameters models (Figure 4). This empirical finding serves as a basis for our theory in §4.

Takeaway 2 (b). As a corollary to Takeaway 2, Figure 3 shows that the best performance is not only achieved when $\beta_1 = \beta_2$, but also improves as the two values become closer. Among 500 runs on 160M-parameter models, we observe a clear correlation: lower loss is associated with smaller differences between β_1 and β_2 . This suggests that gradient smoothing (β_1) and preconditioner smoothing (β_2) should not be treated as independent operations—optimal performance often arises when they act in concert.

To put to the test our second takeaway in **different training settings**, we consider shorter sequence lengths (512, Figure 12), higher/lower batch sizes (Figure 14 & Figure 15), different data (Fineweb) and absence of weight decay (Fig. 16). See discussion in §3.2.

Standard choice for betas. While in standard deep learning (also Pytorch default) $\beta_2 > \beta_1$ (0.999, 0.9), in language modeling the choice $\beta_1 = 0.9, \beta_2 = 0.95$ is much more common. A lower value for β_2 was shown to help mitigate loss spikes [Cattaneo and Shigida, 2025, Compagnoni et al., 2025], and several recent studies have started to adopt $\beta_1 = \beta_2 = 0.95$ as a default [Zhao et al., 2025, Shah et al., 2025, Zhang et al., 2025]. All our findings confirm this choice for tuning (see e.g. Figure 2), of which we evaluate validity extensively for several values of β_1 .

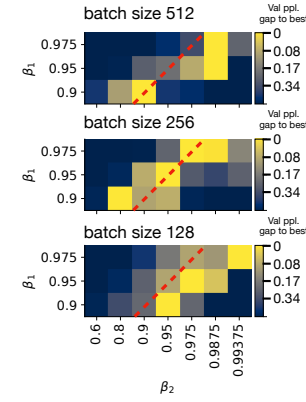


Figure 3: Summary of the results in §B.3. At different batch sizes, for each $\beta_1 \in [0.9, 0.95, 0.975]$, we show the best-performing β_2 (highest score, yellow) and the gap between its performance and that of other options in the grid. We notice high correlation between beta values (e.g., $\beta_2 = 0.9875$ is a terrible option at $\beta_1 = 0.9$, but a good one at $\beta_1 = 0.975$). While results are noisy, notice that $\beta_1 = \beta_2$ never degrades performance more than 0.3 points. In contrast (Table 1), the gap with Signum can be as high as 1.37 points.

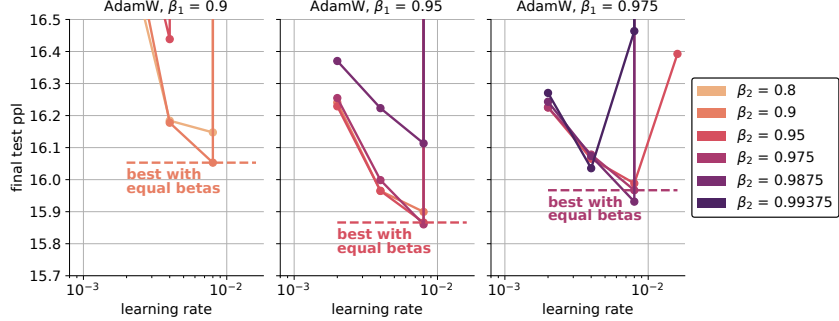


Figure 4: The final validation performance (100M held-out tokens) for 44 trained LMs with 420M parameters trained on 8.2 B SlimPajama tokens (Chinchilla-optimal). **Equal betas yields near-optimal performance.** We use gradient clipping and a batch size of 512 (scaled by 2 compared to Figure 2, as suggested by Zhang et al. [2025]). Sequence length is 2048, weight decay is 0.1. Note that the standard setting (0.9, 0.95) is quite suboptimal here.

3.2 Ablations

Different batch sizes. We find our **Takeaway 2** to be robust to batch size. In the same setting as Figure 2 yet at a slightly lower compute budget due to hardware limitations (2.5B parameters), we find that, even at batch size 128 and 512 the choice $\beta_1 = \beta_2$ yields near-optimal performance. This step involves training 500 models, see §B.3 for visualizations similar to Figure 2 and a discussion.

Different sequence length. We find our **Takeaway 2** to also hold at shorter sequence length of 512 (Figure 12). We note that here performance of Signum is closer to that of Adam compared to Figure 2 – yet, Adam is still superior by a substantial margin (0.7 validation perplexity), **Takeaway 1**. This pattern agrees well with the results in [Zhao et al., 2025], who found other methods to be competitive with Adam at short context lengths. Our experiments in Figure 2 and Figure 16 suggest that Adam performance particularly shines at higher sequence lengths.

Different data and weight decay. In Figure 16 we test both **Takeaway 1** and **Takeaway 2** on Fineweb [Penedo et al., 2024]. We take this opportunity to also deactivate weight decay ($\lambda = 0$), as the optimal Signum learning rates in Figure 2 suggest decoupled weight decay $w = w - \lambda \eta w$ acts differently for the two methods, likely needing different tuning. When deactivated, we still see a substantial gap between Signum and Adam, as well as strong performance with equal betas.

Larger Models We restrict our attention to the SlimPajama dataset and to validation of **Takeaway 2**. Results are presented in Figure 4, comprising 44 full compute-optimal training runs of 410M parameter models, which confirm yet again strong and near-optimal performance at $\beta_1 = \beta_2$.

3.3 Checking for confounders

When comparing Signum with Adam, here are a few confounders that might affect results:

The value of ϵ in Adam was shown to be important for numerical stability, and might affect performance [Yuan and Gao, 2020]. We show in Table 2 that one can choose an extremely small ϵ value in our setting. We cross-check the impact of including an ϵ factor in Signum: we found that little can be gained from this strategy (Figure 5). In short, we found that ϵ is not a crucial parameter in our setup. This is also linked to our findings on adaptive mollifiers, cf. §4.

Initialization of moving average parameters. In Figure 5 we also ablate on initialization of the moving average in Signum and found no substantial differences. We perform this same ablation for Adam and report comprehensive results with seeds in §B.5.

Bias correction. While bias correction in Adam is helpful in early training, final validation performance is almost unchanged, see the full training curve and results with seeds in §B.5.

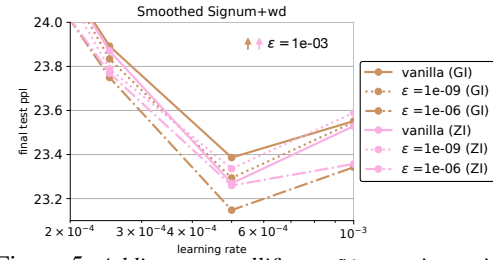


Figure 5: Adding an ϵ mollifier to **Signum**, i.e., using $m_k / (\sqrt{m_k^2 + \epsilon})$ offered little to no improvement. We also test both zero initialization (ZI) and gradient initialization (GI) for m , and find similar results with no significant improvement. $\epsilon = 1e-3$ is significantly worse, hence is not shown. Similar finding: Figure 7.

Table 2: Effect of ϵ in AdamW—other parameters optimally tuned for $\epsilon = 10^{-8}$ (setting: Figure 2). All values between $\epsilon \in [10^{-6}, 10^{-15}]$ result in a similar validation perplexity.

	$\epsilon = 1e - 3$	$\epsilon = 1e - 6$	$\epsilon = 1e - 8$	$\epsilon = 1e - 10$	$\epsilon = 1e - 12$	$\epsilon = 1e - 15$
Val ppl	23.34 ± 0.31	21.56 ± 0.19	21.86 ± 0.21	21.87 ± 0.04	21.89 ± 0.2	21.91 ± 0.18

4 New Viewpoints of Adam

We now show that restricting to the case $\beta_1 = \beta_2 = \beta$ yields a useful interpretation of Adam. Since the Adam update is coordinate-wise, it suffices to analyze a single scalar gradient $g_k \in \mathbb{R}$. Moreover, ablations (Table 2, Table 3) indicate that neither the ϵ -term nor the bias correction significantly affect performance. Thus, for clarity, we set $\epsilon = 0$ and study the simplified Adam update:

$$d_k = \frac{\text{EMA}_\beta[g_k]}{\sqrt{\text{EMA}_\beta[g_k^2]}}. \quad (2)$$

We next rewrite the update in a form that explicitly highlights the role of variance.

Proposition 1. *Let $m_k = \text{EMA}_\beta[g_k]$. Then the update (2) admits the equivalent representation:*

$$d_k = \frac{m_k}{\sqrt{m_k^2 + \beta \text{EMA}_\beta[(m_{k-1} - g_k)^2]}}. \quad (3)$$

This shows that the denominator depends on the exponential moving average of the squared deviation between the momentum m_{k-1} and the incoming gradients g_k , with an **interesting multiplier** β . As we demonstrate in the next section, this quantity is in fact an online estimator of the gradient variance.

Comparison with Balles and Hennig [2018]. Setting $\beta_1 = \beta_2$, a choice that was not common⁵ at the time of [Balles and Hennig \[2018\]](#) allows for precise calculations and claims around variance estimation. In particular, the quantity $\text{EMA}_{\beta_2}[g_k^2] - \text{EMA}_{\beta_1}[g_k]^2$ allows for a precise variance interpretation only for the case $\beta_1 = \beta_2$: we prove in §C.2 that for any $a, b, \gamma \in \mathbb{R}$ and $\tau \in (0, 1)$, the representation

$$d_k = \frac{m_k}{\sqrt{m_k^2 + \gamma \text{EMA}_\tau[(am_{k-1} - bg_k)^2]}}$$

holds for Adam *if and only if* $\beta_1 = \beta_2$. For a proof, see §C.2 in the appendix. In other words, this shows that linking Adam to variance estimation can only be done precisely for the case of equal betas.

4.1 Adam Estimates Mean and Variance using Variational Inference

We now show that Adam admits a natural interpretation as an online variational inference method, in which

$$m_k := \text{EMA}_\beta[g_k] \quad \text{and} \quad \sigma_k := \beta \text{EMA}_\beta[(m_{k-1} - g_k)^2]$$

correspond to online estimates of the mean and variance of the stochastic gradients. We reintroduce Adam through this lens.

Suppose we are given a sequence of stochastic gradients $\{g_1, \dots, g_k\}$, where each g_k is sampled from an unknown Gaussian distribution whose mean and variance may vary with k . Rather than taking steps directly along these noisy gradients, we aim to estimate their mean and variance online and use these estimates to define a more informed search direction.

At iteration k , let (m_k, σ_k^2) denote our current estimates of the gradient mean and variance, respectively. Upon receiving a new gradient sample $g_{k+1} \sim \mathcal{N}(m, \sigma^2)$ with unknown (m, σ^2) , we wish to update our estimates to $(m_{k+1}, \sigma_{k+1}^2)$ so that it becomes more *likely* that g_{k+1} was drawn from $\mathcal{N}(m_{k+1}, \sigma_{k+1}^2)$. Since we also expect the underlying distribution to vary slowly over time, we prefer that $\mathcal{N}(m_{k+1}, \sigma_{k+1}^2)$ remain close to the previous estimate $\mathcal{N}(m_k, \sigma_k^2)$. These two goals—fitting the new observation and ensuring smooth updates—can be traded off via a regularized maximum likelihood problem:

$$\min_{m, \sigma^2 \geq 0} -\log p(g_{k+1} | m, \sigma^2) + \lambda \text{KL}(\mathcal{N}(m_k, \sigma_k^2) \| \mathcal{N}(m, \sigma^2)), \quad (4)$$

⁵Default parameters have for long been $\beta_1 = 0.9$, $\beta_2 = 0.999$, see <https://docs.pytorch.org/docs/stable/generated/torch.optim.Adam.html>.

where $p(g_{k+1} | m, \sigma^2)$ is the Gaussian likelihood, $\lambda \geq 0$ is a regularization parameter, and KL denotes the Kullback–Leibler divergence:

$$-\log p(g_{k+1} | m, \sigma^2) = \frac{1}{2} \log \sigma^2 + \frac{1}{2\sigma^2} (g_{k+1} - m)^2, \quad (5)$$

$$\text{KL}(\mathcal{N}(m_k, \sigma_k^2) \| \mathcal{N}(m, \sigma^2)) = \frac{1}{2} \left[\frac{\sigma_k^2}{\sigma^2} + \frac{(m_k - m)^2}{\sigma^2} - 1 - \log \left(\frac{\sigma_k^2}{\sigma^2} \right) \right]. \quad (6)$$

The following result characterizes the solution of (4), showing that the moving averages used in Adam correspond exactly to an instance of online variational inference:

Theorem 4.1. Let $\beta = \frac{1}{1+\lambda}$. Then the solution to the optimization problem (4) is given by

$$m_{k+1} = \beta m_k + (1 - \beta) g_{k+1} = \text{EMA}_\beta(g_{k+1}), \quad (7)$$

$$\sigma_{k+1}^2 = \beta \sigma_k^2 + \beta(1 - \beta)(m_k - g_{k+1})^2 = \beta \text{EMA}_\beta((m_k - g_{k+1})^2). \quad (8)$$

As a consequence, the Adam update direction in (3) can be rewritten as

$$d_k = \frac{m_k}{\sqrt{m_k^2 + \beta \text{EMA}_\beta((m_{k-1} - g_k)^2)}} = \frac{m_k}{\sqrt{m_k^2 + \sigma_k^2}} = \frac{\text{sign}(m_k)}{\sqrt{1 + \sigma_k^2/m_k^2}}. \quad (9)$$

This shows that Adam may be interpreted as an *adaptive mollified* variant of Signum, where the mollification depends on the local noise-to-signal ratio. This mollified viewpoint aligns well with one of the first papers on understanding Adam [Balles and Hennig, 2018], as discussed after Proposition 1.

Using these insights, we can better formalize the *noise-to-signal* interpretation of Adam [Balles and Hennig, 2018]. Let the quantity m_k/σ_k denote the signal-to-noise ratio (SNR). We show that Adam can be viewed as a steepest descent method whose trust region is modulated by the SNR.

To build this connection, consider first the Signum update. It corresponds to the steepest descent direction under an ℓ_∞ -norm constraint [Balles and Hennig, 2018], solving

$$-\text{sign}(m_k) = \underset{\theta \in \mathbb{R}}{\operatorname{argmin}} -m_k \cdot \theta \quad \text{subject to } |\theta| \leq 1. \quad (10)$$

That is, Signum selects the direction most aligned with $-m_k$ within a unit trust region.

In contrast, Adam can be interpreted as a steepest descent method with a variable trust region, defined by the (inverse) signal-to-noise ratio:

$$-\frac{\text{sign}(m_k)}{\sqrt{1 + \sigma_k^2/m_k^2}} = \underset{\theta \in \mathbb{R}}{\operatorname{argmin}} -m_k \cdot \theta \quad \text{subject to } |\theta| \leq \frac{1}{\sqrt{1 + \sigma_k^2/m_k^2}}. \quad (11)$$

Here, the effective step size shrinks when the noise dominates the signal, and expands toward 1 as uncertainty decreases. In this sense, Adam adapts its update magnitude according to a confidence-weighted trust region.

5 Why an adaptive trust region? Insights from heterogeneous quadratics

While our theoretical analysis in §4 offers a new perspective on Adam, it is not tied to any specific architecture. To enhance intuition and provide a controlled setting for future work, we validate our findings on a simplified model of transformer loss landscapes introduced by Zhang et al. [2024a], building on signal propagation theory [Noci et al., 2022].

As noted in Zhang et al. [2024a], Kunstner et al. [2024], Zhao et al. [2025], the landscape of autoregressive language models is highly heterogeneous: Hessian blocks associated with semantically distinct parameter groups (e.g., normalization layers, embeddings, or softmax-related parameters) exhibit markedly different eigenspectra and thus demand different learning rates. In contrast to homogeneous models (e.g., CNNs), this heterogeneity is where Adam significantly outperforms SGD [cf. Zucchet and Orvieto, 2024].

Figure 6 illustrates this point. On a toy heterogeneous quadratic landscape, tuned Adam with equal β values substantially outperforms tuned SGD with momentum, echoing results from Zhang et al. [2024a]. We also observe that Signum closes much of the gap but still falls short of Adam. This is consistent with our findings in Table 1 for language models.

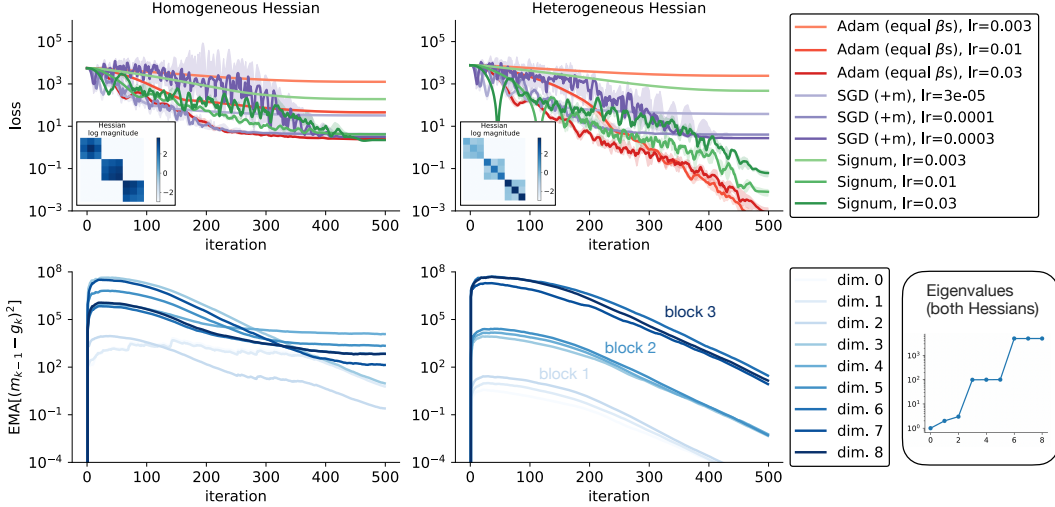


Figure 6: **Top row:** Training performance (median and 25%/75% quantiles over 10 seeds) of SGD, Signum, and Adam on two 9-dimensional convex quadratic problems (\mathcal{D}) inspired by Zhang et al. [2024a]. All optimizers use moving average parameters set to 0.95, with a 10% warmup followed by cosine decay to zero. Both problems share the same Hessian eigenspectrum and have a 3×3 block structure. The landscape on the left is homogeneous, with each block containing both large and small eigenvalues. The landscape on the right is heterogeneous, with each block having eigenvalues of different magnitudes. In this setting, Adam clearly outperforms SGD, with Signum closing part of the gap. **Bottom row:** Dynamics of the variance term in Proposition 1. The value of this term varies both across iterations and across blocks, adapting to the local curvature structure. This adaptive behavior improves performance over Signum in the heterogeneous setting.

In Proposition 1, we showed that the key difference between Signum and Adam lies in the variance correction term $\beta \text{EMA}_\beta[(m_{k-1} - g_k)^2]$ in the denominator. Understanding how this term evolves is essential: it cannot be approximated by a constant. In the second row of Figure 6, we observe that the variance estimate not only varies over time, but also differs in scale across the three blocks—mimicking the parameter groupings in transformer models. This block-wise variation reinforces the idea that the variance term dynamically adapts to the local curvature and cannot be substituted by a fixed value. In Figure 7 and 5, we show a similar effect in heterogeneous quadratic and language models, respectively: replacing $\beta \text{EMA}_\beta[(m_{k-1} - g_k)^2]$ with a fixed constant ϵ cannot provide the same adaptive effect.

6 Conclusion

We have presented an extensive numerical study of Adam, comparing it against several proposed simplifications. Our main finding is that, on generative language modeling tasks, Adam significantly outperforms these simplified variants. Notably, we observe that setting $\beta_1 = \beta_2$ is often optimal or near-optimal. Based on this observation, we recommend Adam with $\beta_1 = \beta_2$ as a simplified model, and we provide a new variational inference interpretation for this setting.

Our findings come with some limitations. First, our numerical experiments fix a grid over the hyperparameters; the results are therefore sensitive to the choice of grid, and different grids may lead to different conclusions. However, for all our hyperparameters, we show explicitly all tuning curves demonstrating that we are always at optimality inside the grid (and not at the edge). Second, while $\beta_1 = \beta_2$ often performs well, we note that at small batch sizes, Figure 3 suggests a slight shift. Finally, although Theorem 4.1 shows that Adam’s two momentum buffers can be interpreted as online estimates of the gradient’s mean and variance, it does not explain why these estimates should be arranged into the quotient used in Adam (9). Lemma 1 in [Balles and Hennig, 2018] can provide a starting point to further dissect this interesting choice and explore alternatives.

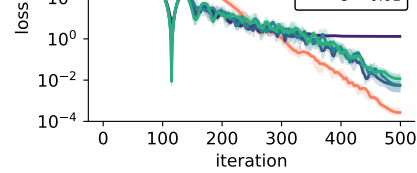


Figure 7: Counterpart of Figure 5 for the heterogeneous quadratic example. We do not observe gains adding a fixed mollifier $m_k / \sqrt{m_k^2 + \epsilon}$. Further, placing inside or outside $\sqrt{\cdot}$ has no qualitative effect.

Acknowledgements

We would like to thank Niccolò Ajroldi, Sam Liang, and Enea Monzio Compagnoni for their valuable feedback. Antonio Orvieto acknowledges the financial support of the Hector Foundation.

References

Lukas Balles and Philipp Hennig. Dissecting Adam: The Sign, Magnitude and Variance of Stochastic Gradients. In *ICML*, 2018.

Jeremy Bernstein and Laker Newhouse. Old optimizer, new norm: An anthology. *arXiv preprint arXiv:2409.20325*, 2024.

Jeremy Bernstein, Yu-Xiang Wang, Kamyar Azizzadenesheli, and Animashree Anandkumar. signsgd: Compressed optimisation for non-convex problems. In *ICML*, 2018.

Stella Biderman, Hailey Schoelkopf, Quentin Gregory Anthony, Herbie Bradley, Kyle O'Brien, Eric Hallahan, Mohammad Aftab Khan, Shivanshu Purohit, USVSN Sai Prashanth, Edward Raff, et al. Pythia: A suite for analyzing large language models across training and scaling. In *ICML*, 2023.

Sid Black, Stella Biderman, Eric Hallahan, Quentin Anthony, Leo Gao, Laurence Golding, Horace He, Connor Leahy, Kyle McDonell, Jason Phang, et al. Gpt-neox-20b: An open-source autoregressive language model. *arXiv preprint arXiv:2204.06745*, 2022.

Matias D. Cattaneo and Boris Shigida. Tuning adam(w): Default β_2 may be too large, 2025. URL https://mdcattaneo.github.io/papers/Cattaneo-Shigida_2025_TuningAdam.pdf.

Xiangning Chen, Chen Liang, Da Huang, Esteban Real, Kaiyuan Wang, Hieu Pham, Xuanyi Dong, Thang Luong, Cho-Jui Hsieh, Yifeng Lu, et al. Symbolic discovery of optimization algorithms. *Advances in neural information processing systems*, 36:49205–49233, 2023.

Aakanksha Chowdhery, Sharan Narang, Jacob Devlin, Maarten Bosma, Gaurav Mishra, Adam Roberts, Paul Barham, Hyung Won Chung, Charles Sutton, Sebastian Gehrmann, et al. Palm: Scaling language modeling with pathways. *Journal of Machine Learning Research*, 24(240):1–113, 2023.

Enea Monzio Compagnoni, Tianlin Liu, Rustem Islamov, Frank Norbert Proske, Antonio Orvieto, and Aurelien Lucchi. Adaptive methods through the lens of SDEs: Theoretical insights on the role of noise. In *ICLR*, 2025.

Tri Dao, Dan Fu, Stefano Ermon, Atri Rudra, and Christopher Ré. Flashattention: Fast and memory-efficient exact attention with io-awareness. *Advances in neural information processing systems*, 35, 2022.

Aaron Grattafiori, Abhimanyu Dubey, Abhinav Jauhri, Abhinav Pandey, Abhishek Kadian, Ahmad Al-Dahle, Aiesha Letman, Akhil Mathur, Alan Schelten, Alex Vaughan, et al. The llama 3 herd of models. *arXiv preprint arXiv:2407.21783*, 2024.

Vineet Gupta, Tomer Koren, and Yoram Singer. Shampoo: Preconditioned stochastic tensor optimization, 2018.

Jordan Hoffmann, Sebastian Borgeaud, Arthur Mensch, Elena Buchatskaya, Trevor Cai, Eliza Rutherford, Diego de Las Casas, Lisa Anne Hendricks, Johannes Welbl, Aidan Clark, et al. Training compute-optimal large language models. *arXiv preprint arXiv:2203.15556*, 2022.

Keller Jordan, Yuchen Jin, Vlado Boza, You Jiacheng, Franz Cesista, Laker Newhouse, and Jeremy Bernstein. Muon: An optimizer for hidden layers in neural networks, 2024. URL <https://kellerjordan.github.io/posts/muon/>.

Andrej Karpathy. Nanogpt, 2022.

Diederik P Kingma and Jimmy Ba. Adam: A method for stochastic optimization. *arXiv preprint arXiv:1412.6980*, 2014.

Frederik Kunstner, Philipp Hennig, and Lukas Balles. Limitations of the empirical fisher approximation for natural gradient descent. In *Advances in Neural Information Processing Systems*, 2019.

Frederik Kunstner, Jacques Chen, Jonathan Wilder Lavington, and Mark Schmidt. Noise is not the main factor behind the gap between sgd and adam on transformers, but sign descent might be. In *ICLR*, 2023.

Frederik Kunstner, Alan Milligan, Robin Yadav, Mark Schmidt, and Alberto Bietti. Heavy-tailed class imbalance and why adam outperforms gradient descent on language models. *Advances in Neural Information Processing Systems*, 2024.

Bingrui Li, Jianfei Chen, and Jun Zhu. Memory efficient optimizers with 4-bit states. *Advances in Neural Information Processing Systems*, 36:15136–15171, 2023.

Aixin Liu, Bei Feng, Bing Xue, Bingxuan Wang, Bochao Wu, Chengda Lu, Chenggang Zhao, Chengqi Deng, Chenyu Zhang, Chong Ruan, et al. Deepseek-v3 technical report. *arXiv preprint arXiv:2412.19437*, 2024.

Hong Liu, Zhiyuan Li, David Hall, Percy Liang, and Tengyu Ma. Sophia: A scalable stochastic second-order optimizer for language model pre-training. *arXiv preprint arXiv:2305.14342*, 2023.

Jingyuan Liu, Jianlin Su, Xingcheng Yao, Zhejun Jiang, Guokun Lai, Yulun Du, Yidao Qin, Weixin Xu, Enzhe Lu, Junjie Yan, et al. Muon is scalable for LLM training. *arXiv preprint arXiv:2502.16982*, 2025.

Ilya Loshchilov and Frank Hutter. Sgdr: Stochastic gradient descent with warm restarts. *arXiv preprint arXiv:1608.03983*, 2016.

Ilya Loshchilov and Frank Hutter. Decoupled weight decay regularization. In *ICLR*, 2019.

Sadhika Malladi, Kaifeng Lyu, Abhishek Panigrahi, and Sanjeev Arora. On the sdes and scaling rules for adaptive gradient algorithms. *Advances in Neural Information Processing Systems*, 2022.

Toan Q Nguyen and Julian Salazar. Transformers without tears: Improving the normalization of self-attention. *arXiv preprint arXiv:1910.05895*, 2019.

Lorenzo Noci, Sotiris Anagnostidis, Luca Biggio, Antonio Orvieto, Sidak Pal Singh, and Aurelien Lucchi. Signal propagation in transformers: Theoretical perspectives and the role of rank collapse. *Advances in Neural Information Processing Systems*, 2022.

Antonio Orvieto, Jonas Kohler, Dario Pavllo, Thomas Hofmann, and Aurélien Lucchi. Vanishing curvature in randomly initialized deep relu networks. In *AISTATS*, pages 7942–7975, 2022.

Razvan Pascanu, Tomas Mikolov, and Yoshua Bengio. On the difficulty of training recurrent neural networks. In *ICML*, 2013.

Guilherme Penedo, Hynek Kydlíček, Loubna Ben allal, Anton Lozhkov, Margaret Mitchell, Colin Raffel, Leandro Von Werra, and Thomas Wolf. The fineweb datasets: Decanting the web for the finest text data at scale. In *The Thirty-eight Conference on Neural Information Processing Systems Datasets and Benchmarks Track*, 2024. URL <https://openreview.net/forum?id=n6SCkn2QaG>.

Thomas Pethick, Wanyun Xie, Kimon Antonakopoulos, Zhenyu Zhu, Antonio Silveti-Falls, and Volkan Cevher. Training deep learning models with norm-constrained lmos. *arXiv preprint arXiv:2502.07529*, 2025.

Alec Radford, Jeffrey Wu, Rewon Child, David Luan, Dario Amodei, Ilya Sutskever, et al. Language models are unsupervised multitask learners. *OpenAI blog*, 1(8):9, 2019.

Sashank J Reddi, Satyen Kale, and Sanjiv Kumar. On the convergence of adam and beyond. In *International Conference on Learning Representations*, 2018.

Ishaan Shah, Anthony M Polloreno, Karl Stratos, Philip Monk, Adarsh Chaluvaraju, Andrew Hojel, Andrew Ma, Anil Thomas, Ashish Tanwer, Darsh J Shah, et al. Practical efficiency of muon for pretraining. *arXiv preprint arXiv:2505.02222*, 2025.

Noam Shazeer. Glu variants improve transformer. *arXiv preprint arXiv:2002.05202*, 2020.

Umut Simsekli, Levent Sagun, and Mert Gurbuzbalaban. A tail-index analysis of stochastic gradient noise in deep neural networks. In *ICML*, 2019.

Daria Soboleva, Faisal Al-Khateeb, Robert Myers, Jacob R Steeves, Joel Hestness, and Nolan Dey. SlimPajama: A 627B token cleaned and deduplicated version of RedPajama, 2023. URL <https://huggingface.co/datasets/cerebras/SlimPajama-627B>.

Jianlin Su, Murtadha Ahmed, Yu Lu, Shengfeng Pan, Wen Bo, and Yunfeng Liu. Roformer: Enhanced transformer with rotary position embedding. *Neurocomputing*, 568:127063, 2024.

Tijmen Tieleman and Geoffrey Hinton. Lecture 6.5-rmsprop, coursera: Neural networks for machine learning. *University of Toronto, Technical Report*, 6, 2012.

Akiyoshi Tomihari and Issei Sato. Understanding why adam outperforms sgd: Gradient heterogeneity in transformers. *arXiv preprint arXiv:2502.00213*, 2025.

Hugo Touvron, Thibaut Lavril, Gautier Izacard, Xavier Martinet, Marie-Anne Lachaux, Timothée Lacroix, Baptiste Rozière, Naman Goyal, Eric Hambro, Faisal Azhar, et al. Llama: Open and efficient foundation language models. *arXiv preprint arXiv:2302.13971*, 2023.

Ashish Vaswani, Noam Shazeer, Niki Parmar, Jakob Uszkoreit, Llion Jones, Aidan N Gomez, Łukasz Kaiser, and Illia Polosukhin. Attention is all you need. *Advances in neural information processing systems*, 30, 2017.

Nikhil Vyas, Depen Morwani, Rosie Zhao, Itai Shapira, David Brandfonbrener, Lucas Janson, and Sham M. Kakade. SOAP: Improving and stabilizing shampoo using adam for language modeling. In *ICLR*, 2025.

Ben Wang and Aran Komatsuzaki. Gpt-j-6b: A 6 billion parameter autoregressive language model. 2021. URL <https://github.com/kingoflolz/mesh-transformer-jax>, page 8, 2022.

Ashia C Wilson, Rebecca Roelofs, Mitchell Stern, Nati Srebro, and Benjamin Recht. The marginal value of adaptive gradient methods in machine learning. *Advances in neural information processing systems*, 30, 2017.

Ruibin Xiong, Yunchang Yang, Di He, Kai Zheng, Shuxin Zheng, Chen Xing, Huishuai Zhang, Yanyan Lan, Liwei Wang, and Tieyan Liu. On layer normalization in the transformer architecture. In *International conference on machine learning*, pages 10524–10533. PMLR, 2020.

Wei Yuan and Kai-Xin Gao. Eadam optimizer: How ϵ impact adam. *arXiv preprint arXiv:2011.02150*, 140, 2020.

Biao Zhang and Rico Sennrich. Root mean square layer normalization. *Advances in Neural Information Processing Systems*, 32, 2019.

Hanlin Zhang, Depen Morwani, Nikhil Vyas, Jingfeng Wu, Difan Zou, Udaya Ghai, Dean Foster, and Sham M. Kakade. How does critical batch size scale in pre-training? In *ICLR*, 2025.

Jingzhao Zhang, Tianxing He, Suvrit Sra, and Ali Jadbabaie. Why gradient clipping accelerates training: A theoretical justification for adaptivity. In *ICLR*, 2020a.

Jingzhao Zhang, Sai Praneeth Karimireddy, Andreas Veit, Seungyeon Kim, Sashank Reddi, Sanjiv Kumar, and Suvrit Sra. Why are adaptive methods good for attention models? *Advances in Neural Information Processing Systems*, 33:15383–15393, 2020b.

Yushun Zhang, Congliang Chen, Tian Ding, Ziniu Li, Ruoyu Sun, and Zhi-Quan Luo. Why transformers need adam: A hessian perspective. In *Neural Information Processing Systems*, 2024a.

Yushun Zhang, Congliang Chen, Ziniu Li, Tian Ding, Chenwei Wu, Diederik P Kingma, Yinyu Ye, Zhi-Quan Luo, and Ruoyu Sun. Adam-mini: Use fewer learning rates to gain more, 2024b.

Rosie Zhao, Depen Morwani, David Brandfonbrener, Nikhil Vyas, and Sham M Kakade. Deconstructing what makes a good optimizer for autoregressive language models. In *ICLR*, 2025.

Nicolas Zucchet and Antonio Orvieto. Recurrent neural networks: vanishing and exploding gradients are not the end of the story. *Advances in Neural Information Processing Systems*, 2024.

Contents

1	Introduction	1
2	Preliminaries and Related Works	3
3	Experiments	4
3.1	Extensive benchmarking at 160M parameters	4
3.2	Ablations	6
3.3	Checking for confounders	6
4	New Viewpoints of Adam	7
4.1	Adam Estimates Mean and Variance using Variational Inference	7
5	Why an adaptive trust region? Insights from heterogeneous quadratics	8
6	Conclusion	9
A	Experimental details	15
A.1	Experiments on SlimPajama – 160M parameters model	16
A.1.1	Sequence Length 2048, Batch size 256, 3.2 B Tokens (6200 gradient steps)	16
A.1.2	Sequence Length 512, Batch size 256, 3.2 B Tokens (24800 gradient steps)	17
A.1.3	Sequence Length 2048, Variable batch size, 2.5 B Tokens	17
A.2	Experiments on SlimPajama – 410M parameters model, 8.2 B tokens	18
A.3	Experiments on Fineweb – 160M parameters model, 3.2B tokens – no weight decay	18
B	Complementary Experimental Results	19
B.1	Tuning for Table 1	19
B.2	Effect of Shorter Sequence Length in Figure 2	21
B.3	Batch size ablation for Figure 2	22
B.4	Figure 2 on Fineweb (no weight decay)	23
B.5	Effect of Bias Correction and Zero Initialization on Adam	23
C	Missing proofs and derivations	24
C.1	Proof of Proposition 1	24
C.2	Generalization of Proposition 1 – Necessity of equal betas for variance interpretation	24
C.3	Proof of Theorem 4.1	26
D	Toy Quadratic Example	27
E	Signal Processing Perspective	28

A Experimental details

For pre-training Transformers on Causal Language Modeling, we build upon the nanoGPT [Karpathy, 2022] implementation, augmenting it with Rotational Positional Embedding [Su et al., 2024], RMSNorm [Zhang and Sennrich, 2019], and SwiGLU [Shazeer, 2020]. All our models have a vocabulary size of 50280 and make use of GPT-NeoX tokenizer [Black et al., 2022]. We adopt an enhanced training recipe, made popular by large language models such as LLaMa [Touvron et al., 2023]. These modifications include: training in bfloat16; employing a linear learning rate warm-up for 10% of the training steps, followed by cosine annealing to $1e-5$. Global norm clipping is used (unless specified or ablated upon) for gradients with norms above 1 (on the raw gradient, as a first step). We have no weight tying between the embedding and the last linear layer. We always report validation perplexity on a separate subset consisting of 100M tokens. Seeds, when provided, are relative to distinct network initialization.

Computational Resources. All our experiments at a 160M parameter scale are performed on a single NVIDIA A100-SXM4-80GB. At compute optimality (most of our experiments) each run takes approximately 5.83 hours. Our runs at a 410M parameter scale are performed on 8 NVIDIA A100-SXM4-80GB GPUs, and each run here takes approximately 4.83 hours. For all our runs, we fill up memory and optimize to minimize the gradient accumulation steps (usually, around 8).

Code. All our runs use the repository

<https://github.com/Niccolo-Ajroldi/plainLM>

Model settings (160M). We use the same configuration as [Biderman et al., 2023]: <https://github.com/EleutherAI/pythia/blob/main/models/160M/pythia-160m.yml>

- *Layers*: 12 Transformer [Vaswani et al., 2017] layers
- *Attention heads*: 12
- *Hidden size*: 768
- *Attention implementation*: Flashattention [Dao et al., 2022].
- *MLP type*: SwiGLU [Shazeer, 2020] with expansion factor 8/3.
- *Backbone*: PreLN transformer [Xiong et al., 2020] with skip connections.
- *Normalization*: RMSnorm [Zhang and Sennrich, 2019] for both Attention and MLP.
- *Position embeddings*: Rotary embeddings (RoPE) to 25% of dimensions ([Su et al., 2024])
- *Initialization*: the MLP and Attention output weights are initialized with variance $0.02/\sqrt{2\#\text{layers}}$ (scaling also similar to [Radford et al., 2019]). All other weights (comprising embeddings) are initialized with a standard deviation of 0.02 (Nguyen and Salazar [2019], Wang and Komatsuzaki [2022], Sec. 2.2). Biases are always initialized at zero.
- *Precision*: Mixed precision FP16 enabled.
- *Dropout*: Disabled for both hidden and attention layers (see also Chowdhery et al. [2023]).

Model settings (410 M). We use the same setting as [Biderman et al., 2023], configuration can be found here: <https://github.com/EleutherAI/pythia/blob/main/models/410M/pythia-410m-deduped.yml>

- *Layers*: 24 Transformer layers
- *Attention heads*: 16
- *Hidden size*: 1024
- Other settings as 160M parameters.

A.1 Experiments on SlimPajama – 160M parameters model

On the Cerebras SlimPajama-627B [Soboleva et al., 2023] dataset: <https://huggingface.co/datasets/cerebras/SlimPajama-627B> at a 160M scale we present three experimental sections:

- Section A.1.1 – core setting, ablating on **all optimizers**.
- Section A.1.2 – ablating on a **smaller sequence length**.
- Section A.1.3 – ablating at **different batch sizes**.

A.1.1 Sequence Length 2048, Batch size 256, 3.2 B Tokens (6200 gradient steps)

This setup comprises a total of 582 full training runs. We always use warm-up (10%) and cosine anneal until a learning rate of $1e - 5$. This setting is Chinchilla-optimal (20 tokens/parameter).

λ here denotes the weight decay, always decoupled [Loshchilov and Hutter, 2019].

Core experiments: These are the core experimental results for this setting.

- **SGD** with momentum β and **global norm clipping** to 1 (Gclip, dampening to $1 - \beta$)
— 84 full runs (Figure 8, top).

$$\begin{aligned} (\eta, \beta, \lambda) \in & [2.0, 1.0, 0.5, 0.25, 0.125, 0.0625, 0.03125] \\ & \times [0.9875, 0.975, 0.95, 0.9] \\ & \times [0, 1e - 3, 1e - 4]. \end{aligned}$$

- **SGD** with momentum β with (1) **global norm clipping** of raw gradient to 1 (Gclip) and (2) **coordinate clipping** (Cclip) to 1 after momentum is applied. Dampening is set to $1 - \beta$, λ (weight decay) is set to 0, as the previous point revealed decreasing performance on SGD
— 24 full runs (Figure 8, bottom).

$$\begin{aligned} (\eta, \beta, \lambda) \in & [2.0, 1.0, 0.5, 0.25, 0.125, 0.0625] \\ & \times [0.9875, 0.975, 0.95, 0.9] \end{aligned}$$

- **SGD** with momentum β (vanilla, dampening to $1 - \beta$, **no clipping**). $\lambda = 0$ (weight decay).
— 28 full runs (Figure 9)

$$\begin{aligned} (\eta, \beta) \in & [0.25, 0.125, 0.0625, 0.03125, 0.015625, 0.0078125, 0.00390625] \\ & \times [0.9875, 0.975, 0.95, 0.9] \end{aligned}$$

- **Adam** with global norm clipping to 1 and with $\lambda = 0.1$ (weight decay) and $\epsilon = 1e - 8$ (usual Pytorch setup, see also Biderman et al. [2023]).
— 200 full runs (Figure 2)

$$\begin{aligned} (\eta, \beta_1, \beta_2) \in & [0.016, 0.008, 0.004, 0.002, 0.001] \\ & \times [0.9875, 0.975, 0.95, 0.9, 0.8] \\ & \times [0.996875, 0.99375, 0.9875, 0.975, 0.95, 0.9, 0.8, 0.6] \end{aligned}$$

- **RMSprop** implemented using the AdamW Pytorch class using $\beta_1 = 0$. We again use $\lambda = 0.1$ (weight decay) and $\epsilon = 1e - 8$.
— 48 full runs (Figure 10).

$$\begin{aligned} (\eta, \beta_2) \in & [0.004, 0.002, 0.001, 0.0005, 0.00025, 0.000125] \\ & \times [0.9875, 0.975, 0.95, 0.9, 0.8, 0.6, 0.4, 0.0] \end{aligned}$$

- **Signum** with weight decay $\lambda = 0.1$ as also suggested by [Zhao et al., 2025] (their Figure 5, top left panel). We **ablate on presence of global norm gradient clipping** (to norm 1).
— 70 full runs (Figure 2).

$$\begin{aligned} (\eta, \beta, \text{clip}) \in & [0.004, 0.002, 0.001, 0.0005, 0.00025, 0.000125, 0.0000625] \\ & \times [0.9875, 0.975, 0.95, 0.9, 0.8] \\ & \times [\text{True}, \text{False}] \end{aligned}$$

Note that Signum with and without gradient clipping are two different methods: here, clipped gradients are first averaged and only then the sign is taken. Instead, clipping on the EMA of signed gradients (next method) should have no effect (apart from non-determinism).

- **EMASign** with weight decay $\lambda = 0.1$. We ablate on the presence of global norm gradient clipping (to norm 1) *out of mistake*: the two methods are equal!
– 70 runs (35 *duplicate runs*) (Figure 11)

$$\begin{aligned} (\eta, \beta, \text{clip}) &\in [0.001, 0.0005, 0.00025, 0.000125, 0.0000625, 0.00003125, 0.000015625] \\ &\times [0.9875, 0.975, 0.95, 0.9, 0.8] \\ &\times [\text{True}, \text{False}] \end{aligned}$$

Ablations: These ablations were performed to test side-claims in the paper.

- **Adam** with global norm clipping to 1 and $\lambda = 0.1, \beta_1 = \beta_2 = 0.95, \eta = 0.008$ (best setup from Figure 2). We report performance for 3 seeds using different ϵ values.
– 18 *full runs* (Table 2).

$$\epsilon \in [1e-3, 1e-6, 1e-8, 1e-10, 1e-12, 1e-15],$$

and influence of initializing exponential moving averages to zero (default, ZI) or to the stochastic quantity of interest (gradient initialization, GI). At the same time, we try to remove bias correction. These experiments are presented with 3 random initialization seeds:
– 9 *full runs* (Table 3).

- **Signum** with global norm clipping to 1 and $\lambda = 0.1, \beta = 0.95$ (best setting from Figure 2): we ablate on fixed mollifiers for zero-initialized (ZI) or gradient-initialized (GI) momentum. The mollified we study is $m_k/(\sqrt{m_k} + \epsilon)$:

$$(\eta, \epsilon) \in [0.001, 0.0005, 0.00025, 0.000125] \times [1e-3, 1e-6, 1e-9]$$

– 12 *full runs* (Table 2).

We additionally test the influence of ZI vs. GI with three random seeds at $\epsilon = 0$.

– 5 *full runs* (Table 3).

Other: for the best-performing variants of core experiments, we initialize the model with two other random seeds. This accounts for

– 14 *additional full runs* (Table 1).

A.1.2 Sequence Length 512, Batch size 256, 3.2 B Tokens (24800 gradient steps)

This setup comprises a total of 55 full training runs. We test our core claims (Signum underperforms Adam, $\beta_1 = \beta_2$ works well) at a smaller sequence length. Setting is exactly the same as §A.1.1 for all methods, unless stated otherwise.

- **Adam**, we limit this ablation to $\beta_1 = 0.95$,

$$(\eta, \beta_2) \in [0.001, 0.002, 0.004, 0.008, 0.016] \times [0.99375, 0.9875, 0.975, 0.95, 0.9, 0.8]$$

– 25 *full runs* (Figure 12).

- **Signum**, we do a full ablation using global norm gradient clipping to 1.

$$(\eta, \beta) \in [0.0000625, 0.000125, 0.00025, 0.0005, 0.001, 0.002] \times [0.9875, 0.975, 0.95, 0.9, 0.8]$$

– 30 *full runs* (Figure 12).

A.1.3 Sequence Length 2048, Variable batch size, 2.5 B Tokens

We use here a slightly reduced token budget (2.5B, 20 tokens for every non-embedding parameter) and run the same Adam tuning experiment presented in Figure 2 for batch size 256. We actually run this experiment again at a batch size of 256, and test batch sizes of 128 and 512 reducing or doubling the number of steps accordingly (same token budget). The sequence length is still 2048, and the dataset SlimPajama. Due to the reduced number of tokens, each run takes approximately 4.7 hours on our hardware. We implement variation of batch size using gradient accumulation (4, 8, 16) at a micro-batch size of 32 sequences. This setup comprises a total of 500 full training runs.

Adam with $\lambda = 0.1$ (weight decay) and $\epsilon = 1e-8$ (usual setup, see Biderman et al. [2023]), we clip gradients to global norm 1.

- For batch size 256:

$$\begin{aligned}
(\eta, \beta_1, \beta_2) \in & [0.016, 0.008, 0.004, 0.002, 0.001] \\
& \times [0.9875, 0.975, 0.95, 0.9, 0.8] \\
& \times [0.996875, 0.99375, 0.9875, 0.975, 0.95, 0.9, 0.8, 0.6]
\end{aligned}$$

- For batch size 128 and 512:

$$\begin{aligned}
(\eta, \beta_1, \beta_2) \in & [0.0005, 0.001, 0.0014, 0.002, 0.0028, 0.004, 0.0056, 0.008, 0.0112, 0.016] \\
& \times [0.975, 0.95, 0.9] \\
& \times 1 - [4, 2, 1, 0.5, 0.25] \cdot (1 - \beta_1) \quad (\text{i.e. 3 higher and 2 lower values in grid})
\end{aligned}$$

Note that here we overturned the learning rate, the reason for this is the square root scaling law in [Malladi et al. \[2022\]](#), [Compagnoni et al. \[2025\]](#): if batch size scales by 2, learning rate should scale as $\sqrt{2}$. We see in §B.3 that this indeed seems to hold true, yet noise prevents us from making precise verification claims.

– 500 full runs (§B.3).

A.2 Experiments on SlimPajama – 410M parameters model, 8.2 B tokens

All our experiments here use the Cerebras SlimPajama-627B [[Soboleva et al., 2023](#)] dataset: <https://huggingface.co/datasets/cerebras/SlimPajama-627B>. We focus on evaluating whether $\beta_1 = \beta_2$ yields good performance in this settings. We scale up the batch size by a factor 2 compared to Section A.1, as suggested by [[Zhang et al., 2025](#)]. We perform our experiments at compute optimality (8.2B tokens, 20 tokens per parameter).

Adam with $\lambda = 0.1$ (weight decay) and $\epsilon = 1e - 8$ (usual setup, see [Biderman et al. \[2023\]](#)), we clip gradients to global norm 1:

- $\beta_1 = 0.9$

$$(\eta, \beta_2) \in [0.016, 0.008, 0.004, 0.002] \times [0.95, 0.9, 0.8]$$

- $\beta_1 = 0.95$

$$(\eta, \beta_2) \in [0.016, 0.008, 0.004, 0.002] \times [0.9875, 0.975, 0.95, 0.9]$$

- $\beta_1 = 0.975$

$$(\eta, \beta_2) \in [0.016, 0.008, 0.004, 0.002] \times [0.99375, 0.9875, 0.975, 0.95]$$

– 44 full runs (Figure 4).

A.3 Experiments on Fineweb – 160M parameters model, 3.2B tokens – no weight decay

While testing our claims on a different dataset, we also crucially *remove weight decay* here. Our setting is otherwise identical to that of §A.1.1: Sequence length is 2048, batch size is 256, model has 160 parameters and we train on 3.2B tokens from Fineweb [[Penedo et al., 2024](#)] <https://huggingface.co/datasets/HuggingFaceFW/fineweb>.

- **Adam** with $\lambda = 0$ (no weight decay!) and $\epsilon = 1e - 8$ (usual setup, see [Biderman et al. \[2023\]](#)). We clip gradients to global norm 1.

$$\begin{aligned}
(\eta, \beta_1, \beta_2) \in & [0.032, 0.016, 0.008, 0.004, 0.002, 0.001] \\
& \times [0.975, 0.95, 0.9] \\
& \times [0.9875, 0.975, 0.95, 0.9, 0.8]
\end{aligned}$$

– 90 full runs (Figure 16)

- **Signum** with $\lambda = 0$ (no weight decay) as also suggested by [[Zhao et al., 2025](#)] (Figure 5, top left panel). We clip gradients to global norm 1.

$$\begin{aligned}
(\eta, \beta) \in & [0.004, 0.002, 0.001, 0.0005, 0.0000625, 0.00025, 0.000125] \\
& \times [0.975, 0.95, 0.9]
\end{aligned}$$

– 24 full runs (Figure 16).

B Complementary Experimental Results

The results in this section complement the discussion in §3. We organize them in 5 subsections, and report all technical details in §A.

- §B.1 outlines all hyperparameter tuning curves for the setting in Table 1 for SGD (with/without clipping and with/without weight decay) – Figure 8 and 9, RMSprop without momentum – Figure 10, and momentum on top of SignSGD – Figure 11.
- §B.2 validates that $\beta_1 = \beta_2$ is a strong-performing option for Adam at a shorter sequence length. Here, we also show that Signum performance is still suboptimal (cf. Figure 2).
- §B.3 validates that $\beta_1 = \beta_2$ is a strong-performing option for Adam across different batch-sizes. This data, comprising training 500 models, is summarized in Figure 3.
- §B.4 reproduces the Signum-Adam gap on Fineweb [Penedo et al., 2024]. Compared to Figure 2 and the settings above, *here we compare at zero weight decay to eliminate this additional confounder*.
- §B.5 confirms on the validity of our findings when ablating on nuances of Signum and Adam such as initialization and bias correction. These findings complement §3.3.

B.1 Tuning for Table 1

Setup Summary. 160 M parameters LM on SlimPajama, trained for 3.2 B tokens at a batchsize of 256×2048 sequence length.

Comment. Our objective here is to tune to best, despite the combinatorially exploding number of options, our methods in Table 1. Details regarding our hyperparameters grid and model configurations are reported in §A. We remind that tuning for Signum and Adam is presented directly in the main paper as Figure 2. **All figures below show optimal tuning jointly in learning rate and momentum space.** While tuning for RMSprop and momentum on SignSGD is straightforward, SGD requires more attention: we found that removing weight decay was always beneficial when global norm clipping the raw gradient, hence we adopt this option also for the non-clipped variant, and for the variant that includes an additional coordinate clipping step after applying momentum. We believe this is due to the decoupled nature of weight decay, combined with the high learning rates required for good performance in SGD.

Finalizing Table 1. After careful tuning, we select for each method the best configuration (given by figures below) and run two additional seeds to report final results with 2-sigma confidence bars.

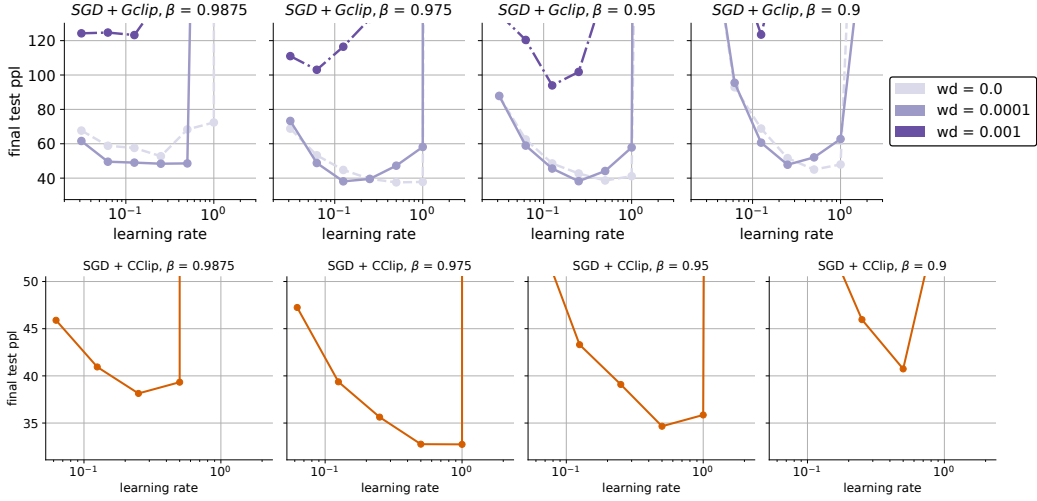


Figure 8: **(top) SGD with global norm clipping.** We found it beneficial to remove weight decay: the best setting achieves 37.53 ppl, while a slightly larger wd leads to 38.11. a weights decay of 0.001 is too large and yields 93.7 best validation perplexity. **(bottom) SGD with global norm clipping on raw gradients, followed by coordinate clipping on momentum.** We remove weight decay as suggested by the top plot. We observe an improvement of 5 perplexity points.

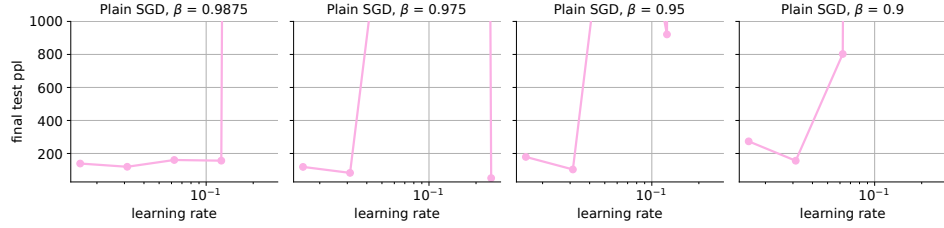


Figure 9: **SGD without coordinate-wise clipping at zero weight decay (as suggested by Figure 8).**

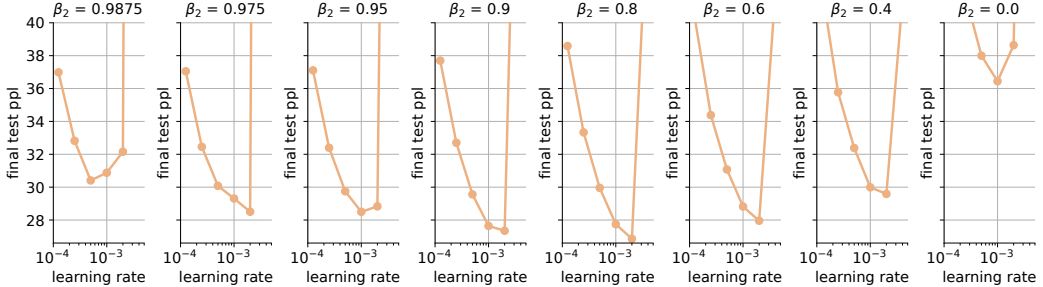


Figure 10: **RMSprop with decoupled weight decay 0.1.** Implemented with Pytorch AdamW setting $\beta_1 = 0$.

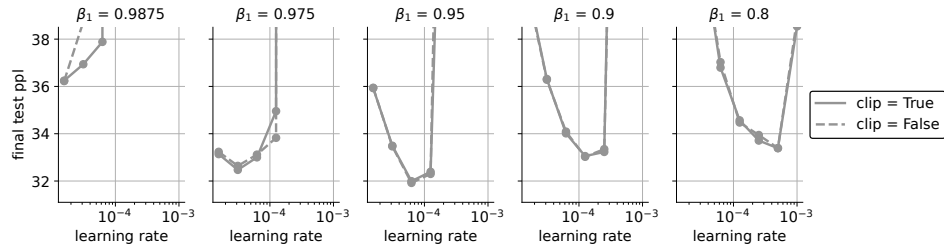


Figure 11: **Momentum on SignSGD with decoupled weight decay.** We implement this just for completeness to show that it is performing worse than Signum. Clipping has mathematically no effect (we did not notice at first, so we show the result anyways).

B.2 Effect of Shorter Sequence Length in Figure 2

We run part of the experiments in Figure 2 at a lower sequence length (512), for a batch size of 256 sequences (as Figure 2). The model here still sees 3.2B tokens (compute optimal), but number of effective optimizer steps is 4 times bigger compared to the 2048 sequence length setting. While we still observe a sizeable gap between Signum and Adam, we note that this is smaller compared to Figure 2, as noted also by Zhao et al. [2025] in a similar setting.

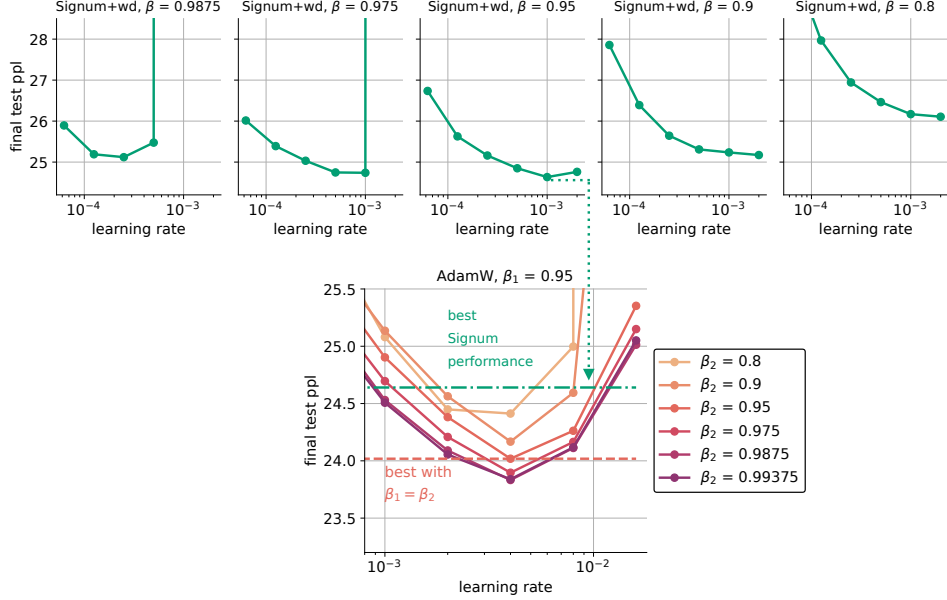


Figure 12: **AdamW vs Signum**, same setting as Figure 2, but at a smaller sequence length (512).

B.3 Batch size ablation for Figure 2

We run part of the experiments in Figure 2 at a lower and higher batch size. All other details remain the same and are summarized in §A – except for the number of steps performed: due to limitations in our resources, we chose here to train models for 2.5B tokens – i.e. a slightly undertrained setting (optimal would be 3.2B). In line with [Malladi et al., 2022, Compagnoni et al., 2025] we consider half-steps when tuning. All experiments use a weight decay of 0.1.

Despite some imperfections and noise in performance, we notice that $\beta_1 = \beta_2$ is a strong choice even at different batch sizes, our Takeaway 2.

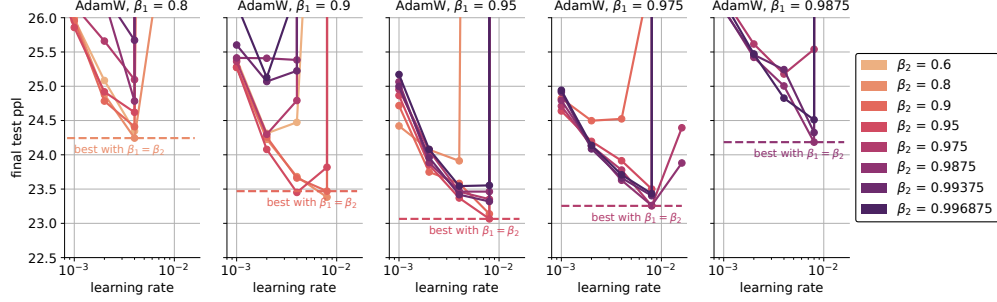


Figure 13: *Adam, batch size 256* trained for 2.5B tokens. Other settings are same setting as Figure 2.

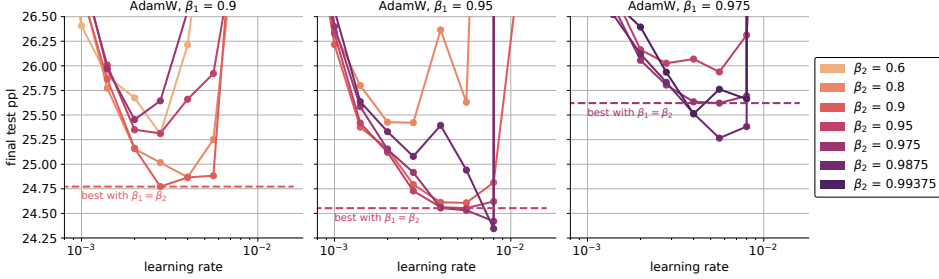


Figure 14: *Adam, batch size 512* trained for 2.5B tokens. Other settings are same setting as Figure 2.

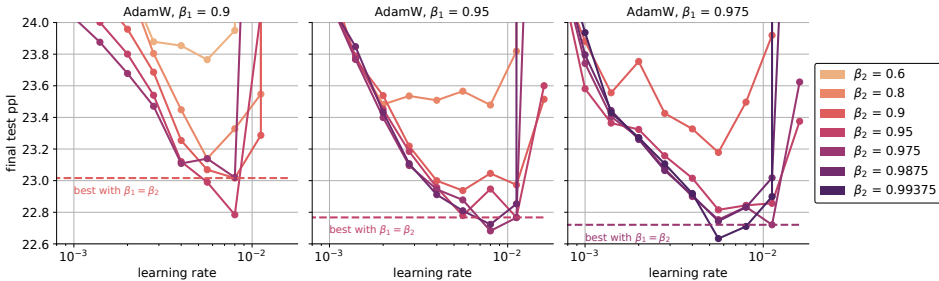


Figure 15: *Adam, batch size 128* trained for 2.5B tokens. Other settings are same setting as Figure 2.

B.4 Figure 2 on Fineweb (no weight decay)

Finally, we evaluate our findings – both strong performance of equal β s in Adam and substantial gap with Signum on a different dataset (Fineweb [Penedo et al., 2024]). All other experiments in this paper are performed on SlimPajama. To add an additional axis of variation compared to previously presented settings, we here remove weight decay from all methods.

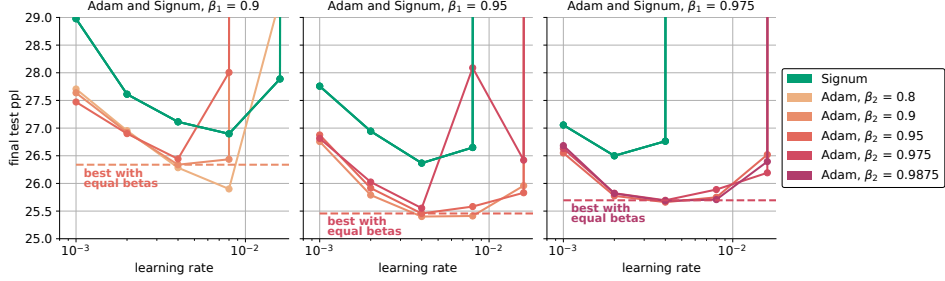


Figure 16: *Adam and Signum (no weight decay) on Fineweb*. Other settings are same as Figure 2. For visualization purposes, here we rescaled the visualized learning rate of Signum by a factor ~ 10 .

B.5 Effect of Bias Correction and Zero Initialization on Adam

The findings below complement our discussion in §3.3.

Table 3: *ZI* denotes Zero init of EMA parameters, *GI* denotes init of EMA parameters to the measurement at first iteration, *BC* denotes Bias Correction. *Not doing ZI* means we initialize m and v at g_0 and g_0^2 respectively. Default for Adam is ZI and BC. Default for Signum+WD is less clear. We found that initialization does not affect much performance in Signum, yet it does in Adam. Performing bias correction is not as important as initialization in Adam. All other parameters in this ablation are fixed to the optimal ones found in default settings for BC and ZI.

	Adam (+ZI+BC)	Adam (+ZI-BC)	Adam (+GI-BC)	Signum (+GI)	Signum (+ZI)
Val ppl	21.86 ± 0.21	21.89 ± 0.16	22.58 ± 0.35	23.23 ± 0.16	23.30 ± 0.25

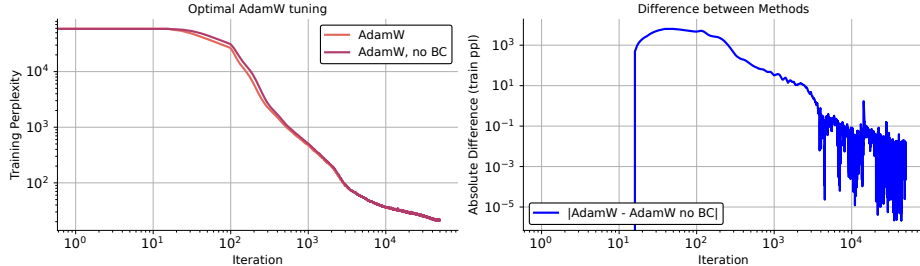


Figure 17: *Effect of eliminating bias correction in Adam*. The difference between variants vanishes as iterations progress. Plotted is the average dynamics over 3 random seeds.

C Missing proofs and derivations

C.1 Proof of Proposition 1

Proposition 1. Let $m_k = \text{EMA}_\beta[g_k]$. Then the update (2) admits the equivalent representation:

$$d_k = \frac{m_k}{\sqrt{m_k^2 + \beta \text{EMA}_\beta[(m_{k-1} - g_k)^2]}}. \quad (3)$$

Proof of Proposition 1. For this proof we will use the abbreviation

$$v_k := \text{EMA}_\beta[g_k^2].$$

With this abbreviation the Adam update (2) can be written as

$$d_k = \frac{m_k}{\sqrt{v_k}} = \frac{m_k}{\sqrt{m_k^2 + v_k - m_k^2}}.$$

Next we will show that $v_k - m_k^2 = \beta \text{EMA}_\beta[(m_{k-1} - g_k)^2]$. Indeed by expanding the update of v_{k+1} and m_{k+1} we have that

$$\begin{aligned} v_{k+1} - m_{k+1}^2 &= \beta v_k + (1 - \beta)g_{k+1}^2 - (\beta m_k + (1 - \beta)g_{k+1})^2 \\ &= \beta v_k + (1 - \beta)g_{k+1}^2 - (\beta^2 m_k^2 + (1 - \beta)^2 g_{k+1}^2 + 2\beta(1 - \beta)g_{k+1}m_k) \\ &= \beta v_k - \beta^2 m_k^2 + (1 - \beta)\beta g_{k+1}^2 - 2\beta(1 - \beta)g_{k+1}m_k \\ &= \beta v_k - \beta m_k^2 + \beta m_k^2 - \beta^2 m_k^2 + (1 - \beta)\beta g_{k+1}^2 - 2\beta(1 - \beta)g_{k+1}m_k \\ &= \beta(v_k - m_k^2) + \beta(1 - \beta)m_k^2 + \beta(1 - \beta)g_{k+1}^2 - 2\beta(1 - \beta)g_{k+1}m_k \\ &= \beta(v_k - m_k^2) + \beta(1 - \beta)(m_k - g_{k+1})^2. \end{aligned}$$

By setting $\delta_k = v_k - m_k^2$ we have that

$$\delta_{k+1} = \beta\delta_k + \beta(1 - \beta)(m_k - g_{k+1})^2 = \beta \text{EMA}_\beta[(m_{k-1} - g_k)^2]$$

where we used the definition of the EMA recurrence in (1).

□

C.2 Generalization of Proposition 1 – Necessity of equal betas for variance interpretation

Proposition 2. Adam with hyperparameters $\beta_1, \beta_2 \in (0, 1)$ has update of form

$$\frac{m_k}{\sqrt{m_k^2 + \gamma \text{EMA}_\tau[(am_{k-1} - bg_k)^2]}},$$

for some $a, b, \gamma \in \mathbb{R}$ and $\tau \in (0, 1)$ if and only if $\beta_1 = \beta_2$.

Proof of Proposition 2. Let us expand the expression.

$$\begin{aligned} v_{k+1} - m_{k+1}^2 &= \beta_2 v_k + (1 - \beta_2)g_{k+1}^2 - (\beta_1 m_k + (1 - \beta_1)g_{k+1})^2 \\ &= \beta_2 v_k + (1 - \beta_2)g_{k+1}^2 - [\beta_1^2 m_k^2 + (1 - \beta_1)^2 g_{k+1}^2 + 2\beta_1(1 - \beta_1)m_k g_{k+1}] \\ &= \beta_2 v_k - \beta_1^2 m_k^2 + [(1 - \beta_2) - (1 - \beta_1)^2]g_{k+1}^2 - 2\beta_1(1 - \beta_1)m_k g_{k+1} \end{aligned}$$

The case of equal betas. Notice that if $\beta_1 = \beta_2 = \beta$, then

$$(1 - \beta) - (1 - \beta)^2 = 1 - \beta - (1 + \beta^2 - 2\beta) = 1 - \beta - 1 - \beta^2 + 2\beta = \beta(1 - \beta),$$

and so the expression gets simplified:

$$v_{k+1} - m_{k+1}^2 = \beta v_k - \beta^2 m_k^2 + \beta(1 - \beta)[g_{k+1}^2 - 2m_k g_{k+1}]$$

Now add and subtract βm_k^2 , to get

$$v_{k+1} - m_{k+1}^2 = \beta(v_k - m_{k+1}) + \beta(1 - \beta)[m_k^2 + g_{k+1}^2 - 2m_k g_{k+1}].$$

where the last term is the perfect square $(m_k - g_{k+1})^2$.

The general setting. One might hope for the “stars aligning” into a perfect square also in the general setting. For this to happen, we need to require that the term

$$[(1 - \beta_2) - (1 - \beta_1)^2]g_{k+1}^2 - 2\beta_1(1 - \beta_1)m_k g_{k+1}$$

allows for such a simplification to happen. That is, assume to start from

$$(am_k - bg_{k+1})^2 = a^2m_k^2 - 2abm_k g_{k+1} + b^2g_{k+1}^2.$$

we need

$$b^2 = (1 - \beta_2) - (1 - \beta_1)^2, \quad ab = \beta_1(1 - \beta_1).$$

so

$$a = \frac{\beta_1(1 - \beta_1)}{\sqrt{(1 - \beta_2) - (1 - \beta_1)^2}}.$$

Therefore:

$$\begin{aligned} & \left(\frac{\beta_1(1 - \beta_1)}{\sqrt{(1 - \beta_2) - (1 - \beta_1)^2}} m_k - \sqrt{(1 - \beta_2) - (1 - \beta_1)^2} g_{k+1} \right)^2 \\ &= \frac{\beta_1^2(1 - \beta_1)^2}{(1 - \beta_2) - (1 - \beta_1)^2} m_k^2 + [(1 - \beta_2) - (1 - \beta_1)^2]g_{k+1}^2 - 2\beta_1(1 - \beta_1)m_k g_{k+1} \end{aligned}$$

Therefore, in the general setting, we can write

$$\begin{aligned} v_{k+1} - m_{k+1}^2 &= \beta_2 v_k - \left(\beta_1^2 + \frac{\beta_1^2(1 - \beta_1)^2}{(1 - \beta_2) - (1 - \beta_1)^2} \right) m_k^2 + \\ &+ \left(\frac{\beta_1(1 - \beta_1)}{\sqrt{(1 - \beta_2) - (1 - \beta_1)^2}} m_k - \sqrt{(1 - \beta_2) - (1 - \beta_1)^2} g_{k+1} \right)^2 \end{aligned}$$

Massaging a bit, we get

$$\begin{aligned} v_{k+1} - m_{k+1}^2 &= \beta_2 v_k - \frac{\beta_1^2(1 - \beta_2)}{(1 - \beta_2) - (1 - \beta_1)^2} m_k^2 + \\ &+ \left(\frac{\beta_1(1 - \beta_1)}{\sqrt{(1 - \beta_2) - (1 - \beta_1)^2}} m_k - \sqrt{(1 - \beta_2) - (1 - \beta_1)^2} g_{k+1} \right)^2 \end{aligned}$$

which implies

$$\begin{aligned} v_{k+1} - m_{k+1}^2 &= \beta_2 \left(v_k - \frac{\beta_1^2(1 - \beta_2)}{\beta_2(1 - \beta_2) - \beta_2(1 - \beta_1)^2} m_k^2 \right) + \\ &+ \left(\frac{\beta_1(1 - \beta_1)}{\sqrt{(1 - \beta_2) - (1 - \beta_1)^2}} m_k - \sqrt{(1 - \beta_2) - (1 - \beta_1)^2} g_{k+1} \right)^2. \end{aligned}$$

Therefore, the formula holds true if and only if

$$\frac{\beta_1^2(1 - \beta_2)}{\beta_2(1 - \beta_2) - \beta_2(1 - \beta_1)^2} = 1.$$

That is, if and only if

$$\beta_1^2(1 - \beta_2) = \beta_2(1 - \beta_2) - \beta_2(1 - \beta_1)^2.$$

The condition simplifies, as it reads:

$$\beta_1^2 - \beta_1^2\beta_2 = \beta_2 - \beta_2^2 - \beta_2 - \beta_2\beta_1^2 + 2\beta_1\beta_2.$$

which simplified is

$$\beta_1^2 + \beta_2^2 - 2\beta_1\beta_2 = 0.$$

i.e.

$$(\beta_1 - \beta_2)^2 = 0 \iff \beta_1 = \beta_2.$$

□

C.3 Proof of Theorem 4.1

Theorem 4.1. Let $\beta = \frac{1}{1+\lambda}$. Then the solution to the optimization problem (4) is given by

$$m_{k+1} = \beta m_k + (1 - \beta) g_{k+1} = \text{EMA}_\beta(g_{k+1}), \quad (7)$$

$$\sigma_{k+1}^2 = \beta \sigma_k^2 + \beta(1 - \beta)(m_k - g_{k+1})^2 = \beta \text{EMA}_\beta((m_k - g_{k+1})^2). \quad (8)$$

Proof. Substituting the definitions of Gaussian likelihood and KL divergence (6) into (4) gives the following objective function

$$\min_{m, \sigma^2 \geq 0} F(m, \sigma^2) = \frac{1}{2} \frac{1+\lambda}{\lambda} \log(\sigma^2) + \frac{1}{2\sigma^2} \left[(g - m)^2 + \frac{1}{\lambda} (\sigma_k^2 + (m_k - m)^2) \right] + \text{const.}$$

Stationarity in m : Differentiating in m and setting to zero gives

$$\frac{\partial F}{\partial m} = -\frac{1}{\sigma^2}(g - m) - \frac{1}{\lambda\sigma^2}(m_k - m) = 0.$$

Multiplying by $\lambda\sigma^2$, we get:

$$-\lambda(g - m) - (m_k - m) = 0 \quad \Rightarrow \quad m = \frac{\lambda g + m_k}{1 + \lambda}. \quad (12)$$

Stationarity in σ^2 : Differentiating in σ^2 and setting to zero gives

$$\frac{\partial F}{\partial \sigma^2} = \frac{1}{2} \frac{1+\lambda}{\lambda} \cdot \frac{1}{\sigma^2} - \frac{1}{2\sigma^4} \left[(g - m)^2 + \frac{1}{\lambda} (\sigma_k^2 + (m_k - m)^2) \right] = 0.$$

Multiplying both sides by $2\sigma^4$, and re-arranging gives:

$$\frac{1+\lambda}{\lambda} \sigma^2 = (g - m)^2 + \frac{1}{\lambda} (\sigma_k^2 + (m_k - m)^2).$$

Multiplying through by $\frac{\lambda}{1+\lambda}$ gives

$$\sigma^2 = \frac{\lambda(g - m)^2 + [\sigma_k^2 + (m_k - m)^2]}{1 + \lambda}. \quad (13)$$

Now using $m = \frac{\lambda g + m_k}{1 + \lambda}$ from (12) we have that

$$g - m = \frac{g - m_k}{1 + \lambda}, \quad m_k - m = \frac{\lambda(m_k - g)}{1 + \lambda}.$$

Therefore:

$$(g - m)^2 = \frac{(g - m_k)^2}{(1 + \lambda)^2}, \quad (m_k - m)^2 = \frac{\lambda^2(g - m_k)^2}{(1 + \lambda)^2}.$$

Using the above in the expression for σ^2 in (13), we get:

$$\sigma^2 = \frac{\lambda(g - m_k)^2}{(1 + \lambda)^2} + \frac{\sigma_k^2}{1 + \lambda}.$$

This, together with (12) gives the final solution

$$m_{k+1} = \frac{m_k + \lambda g}{1 + \lambda} \quad \text{and} \quad \sigma_{k+1}^2 = \frac{\sigma_k^2}{1 + \lambda} + \frac{\lambda(g - m_k)^2}{(1 + \lambda)^2}.$$

If we use the standard momentum parameterization, which corresponds to $\beta = \frac{1}{1+\lambda}$ we arrive at the stated results (7) and (8) of the theorem. \square

D Toy Quadratic Example

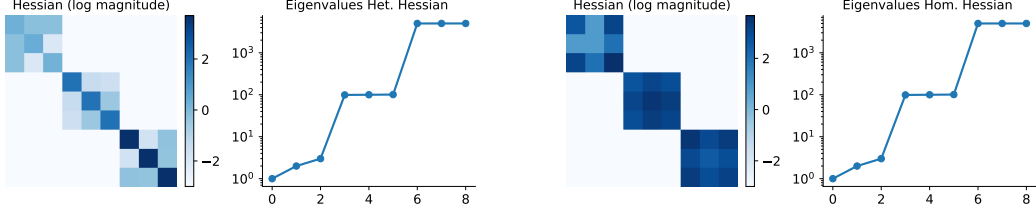


Figure 18: (left) Heterogeneous and (right) Homogeneous Hessian considered in §5.

Our setup here is inspired directly from the results and discussions in [Zhang et al. \[2024a\]](#). Specifically, we consider the loss

$$L(w) = \frac{1}{2} w^\top H w$$

where we construct the Homogeneous and Heterogeneous Hessians using the following procedure:

- We fix the eigenvalues, equal in both cases, to

$$\text{eig}(H_{\text{hom}}) = \text{eig}(H_{\text{het}}) = \{1, 2, 3, 99, 100, 101, 4998, 4999, 5000\}.$$

- We choose both Hessians to be block-diagonal, with blocks of size 3×3 . The homogeneous Hessian has eigenvalues of different magnitude in each block, while the Heterogeneous keeps similar magnitudes in each block.

$$\begin{aligned} \text{H_details_het} &= [[1, 2, 3], [99, 100, 101], [4998, 4999, 5000]] \\ \text{H_details_hom} &= [[1, 99, 4998], [2, 100, 4999], [3, 101, 5000]] \end{aligned}$$

- For each block, we apply a random rotation to the diagonal matrix of eigenvalues, specific to each block. Each rotation is sampled from the Haar measure by decomposition of a random 3×3 positive semidefinite matrix AA^\top , where $A \in \mathbb{R}^{3 \times 3}$ has i.i.d. Gaussian entries.

The result is shown in Figure 18.

Next, to introduce stochasticity in this setting, we simply take the square root of the Hessian to define a 9×9 design matrix X

$$H = X^\top X, \quad X = H^{\frac{1}{2}}$$

and subsample a number (the batchsize) of rows of X at each iteration.

E Signal Processing Perspective

In this last section, we examine Adam through a signal processing lens, to get qualitative insights into its distinction with Signum and other SignSGD with momentum variants. Setting $\beta_1 = \beta_2 = \beta$, we can write the Adam update, without bias correction (see §B.5) as simply

$$d_k = \left(\sqrt{\text{EMA}_\beta[g_k^2]} + \epsilon \right)^{-1} \text{EMA}_\beta[g_k]$$

where $(g_k)_k$ is the gradient signal. One might wonder if this special case allows for a simpler graphical interpretation of Adam. To do this, we consider here fixing the gradient signal, and see how different methods process this signal.

Graphical intuition. We denote by d_k the update of Adam once it sees a gradient signal $(g_i)_{i \leq k}$: and plot its dynamics as a function of a synthetic one-dimensional gradient in Figure 19.

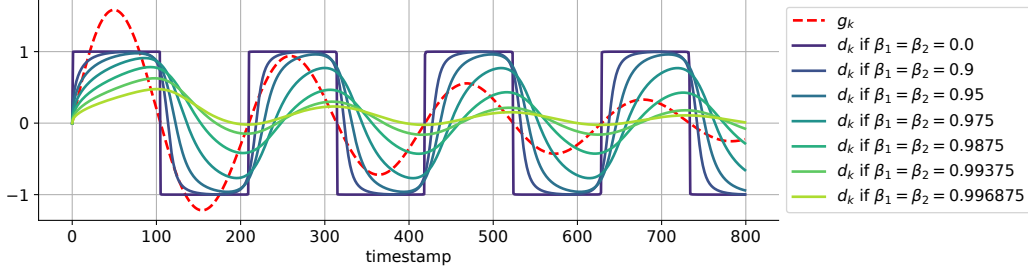


Figure 19: Filtering effect for same $\beta_1 = \beta_2$.

In the example of Figure 19, we chose the synthetic gradient signal

$$g_k = 1.8 \sin(0.03k) \exp(-0.0025k)$$

this is a damped periodic signal plotted in red. Note that this is pure filtering, there is no loss or learning process. We note the following:

1. $\beta_1 = \beta_2 = 0$ is obviously just $\text{sign}(g_k)$. This is plotted for comparison.
2. For any $\beta_1 = \beta_2 \neq 0$, d_k is bounded by 1 in magnitude. Its dynamics however, for e.g. $\beta_1 = \beta_2 > 0$ is smooth and follows more closely the gradient, while being bounded. It is somehow a rescaled version. More on this later.
3. Very interestingly, d_k is blind to the decay term $\exp(-0.0025k)$, the output is perfectly periodic for every $\beta_1 = \beta_2$.

Towards proceeding, note that d_k **cannot be reduced to momentum on the sign or sign on the momentum(Signum)**: both variants actually destroy the signal shape, while d_k maintains the shape of the original signal and has clear invariance properties. The behavior of signSGD with momentum (2 variants) is shown in Figure 20: as one can see, the behavior is drastically different from d_k in Figure 19, an enlargement is shown in Figure 21.

We now try to formalize some of the properties we observe.

Properties. Adam can be seen as a very special operator T on gradient sequences $(g_k)_{k=0}^\infty \in \mathcal{G} \subseteq \ell_\infty$ (with normed vector space structure and notation). We can identify four distinctive properties. $T : (g_k)_{k=0}^\infty \rightarrow (d_k)_{k=0}^\infty$.

1. It is **causal**.
2. It is **invariant to positive scaling**: $T(\alpha \cdot g) = T(g)$, for any $\alpha > 0$.
3. It is **odd**: $T(-g) = -T(g)$.
4. It has **bounded** infinity norm: $\|T(g)\|_\infty \leq 1$ for all $g \in \ell_\infty$.

5. **Density:** For any $b \in [-1, 1]$ and any arbitrary $k > 0$, there exists $(g_k)_{k=0}^\infty$ such that $d_k = b$.

We are amazed by these rich set of properties, thickening our interest in better understanding the properties of Adam mollification, which we study in §4.

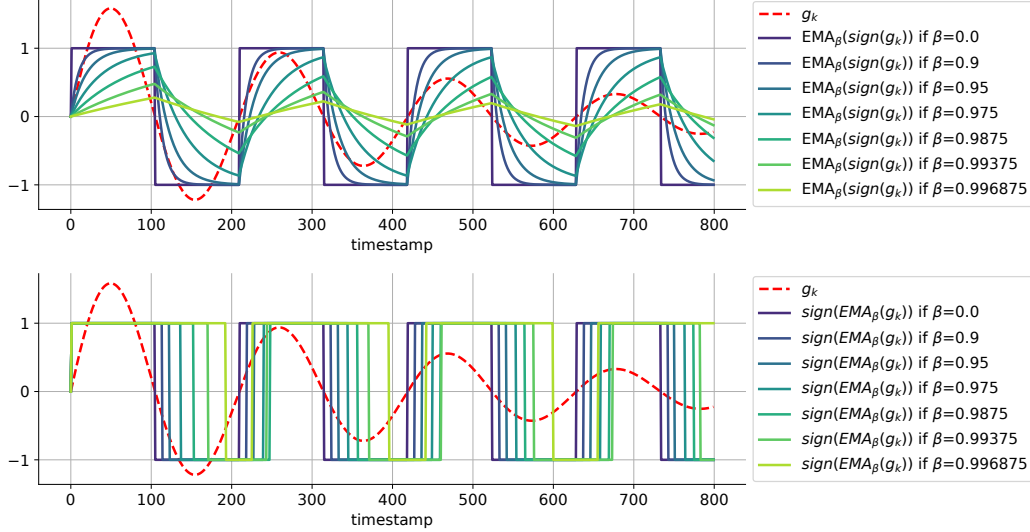


Figure 20: Filtering induced by signSGD with momentum (2 variants, the one below is Signum). Compare with Figure 19.

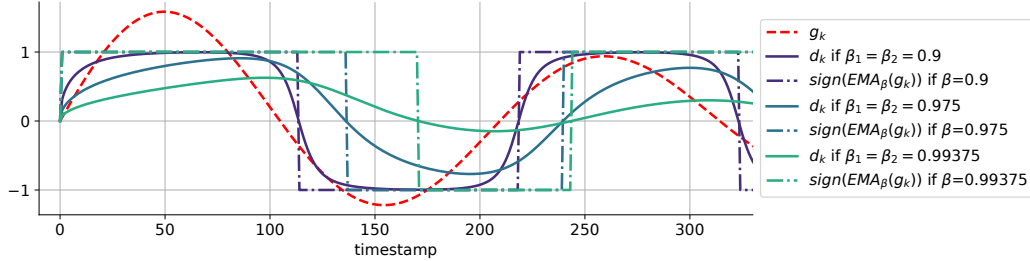


Figure 21: Adam-like filtering compared to sign of EMA (Signum), detail.

We hope this investigation inspires future efforts in understanding these intriguing phenomena and properties. We conclude the paper with a quote, stolen from the Bernt Øksendal masterpiece book on SDEs:

*We have not succeeded in answering all our problems.
The answers we have found only serve to raise a whole set
of new questions. In some ways we feel we are as confused
as ever, but we believe we are confused on a higher level
and about more important things.*

Posted outside the mathematics reading room –Tromsø University